# Drought legacies are short, prevail in dry conifer forests and depend on growth variability

Antonio Gazol[1] | J. Julio Camarero[1] | Raul Sánchez-Salguero[1,2] | Sergio M. Vicente-Serrano[1] | Xavier Serra-Maluquer[1] | Emilia Gutiérrez[3] | Martin de Luis[4] | Gabriel Sanguesa-Barreda[1,5] | Klemen Novak[6,7] | Vicente Rozas[5] | Pedro A. Tíscar[8] | Juan C. Linares[2] | Edurne Martínez del Castillo[4,9] | Montse Ribas[3] | Ignacio García-González[10] | Fernando Silla[11] | Alvaro Camison[12] | Mar Génova[13] | José M. Olano[5] | Ana-Maria Hereş[14,15] | Jorge Curiel Yuste[15,16] | Luis A. Longares[4] | Andrea Hevia[17] | Miquel Tomas-Burguera[18] | J. Diego Galván[19]

[1]Instituto Pirenaico de Ecología (IPE-CSIC), Zaragoza, Spain

[2]Depto. Sistemas Físicos, Químicos y Naturales, Univ. Pablo de Olavide, 41013, Sevilla, Spain

[3]Department of Evolutionary Biology, Ecology and Environmental Sciences, University of Barcelona, Barcelona, Spain

[4]Depto. Geografía y Ordenación del Territorio - IUCA, Univ. Zaragoza, Zaragoza, Spain

[5]EiFAB-iuFOR-EiFAB,-, Campus Duques de Soria, Univ. Valladolid, E-42004-Soria, Spain

[6]University of Ljubljana, Biotechnical Faculty, Department of Wood Science and Technology, Ljubljana, Slovenia

[7]Depto. de Ecología, Universidad de Alicante, Alicante, Spain

[8]Centro de Capacitación y Experimentación Forestal, Cazorla, Spain

[9]Agrotecnio - Av. Rovira Roure 191, 25198 Lleida, Spain

[10]Depto. Botánica, Escola Politécnica Superior de Enxeñaría, Campus Terra, Universidade de Santiago de Compostela, Lugo, Spain

[11]Depto. Biología Animal, Parasitología, Ecología, Edafología y Química Agrícola, Univ. Salamanca, Salamanca, Spain

[12]Ingeniería Forestal y del Medio Natural, Univ. Extremadura, Plasencia, Spain

[13]Depto. Sistemas y Recursos Naturales, Univ. Politécnica de Madrid, Madrid, Spain

[14]Department of Forest Sciences, Transilvania University of Braşov, Şirul Beethoven -1, 500123, Braşov, Romania

[15]Basque Centre for Climate Change (BC3), Sede Building 1, 48940 Leioa, Spain.

[16]IKERBASQUE, Basque Foundation for Science, Bilbao, Bizkaia, Spain

[17]Departamento de Ciencias Agroforestales, Universidad de Huelva, Huelva, Spain

[18]Estación Experimental Aula Dei (EEAD-CSIC), Zaragoza, Spain

[19]Ionplus AG. Lerzenstrasse, Dietikon, Switzerland

**Type of article:** Research article

***Correspondence**: Dr. Antonio Gazol

Instituto Pirenaico de Ecología (IPE-CSIC)

Avda. Montañana 1005, 50059 Zaragoza, Spain

E-mail: agazol@ipe.csic.es; Phone: + 34 976369393 ext. 880041

## Abstract

- The negative impacts of drought on forest growth and productivity last for several years generating legacies, although the factors that determine why such legacies vary across sites and tree species remain unclear.
- We used an extensive network of tree-ring width (RWI, ring-width index) records of 16 tree species from 576 forests, and high-resolution climate and NDVI datasets across Spain during the period 1982–2008 to test the hypothesis that climate conditions and growth features modulate legacy effects of drought on forests. Legacy effects of drought were calculated as the differences between detrended-only RWI and NDVI series (i.e. after removing long-term growth trends) and predicted pre-whitened RWI and NDVI series by a model including drought intensity. Superposed epoch analysis (SEA) was used to estimate whether legacy effects differed from random. Finally, legacy effects were related to water balance, growth persistence and variability, and tree species identity.
- We found a widespread occurrence of drought legacy effects in both RWI and NDVI, but they were seldom significant. According to SEA, first-year drought legacies were negative and different from random in 9% and 5% of the RWI and NDVI series, respectively. The number of significant second- and third-year legacies was substantially lower. Differences between NDVI and RWI legacies indicate that canopy greenness and growth responses to drought are decoupled. We found variations in legacies between tree species with gymnosperms presenting larger first-year drought legacies than angiosperms, which were exposed to less severe droughts. Greater growth variability can explain the presence of first-year RWI legacies in gymnosperms from dry sites despite the relationship between growth variability and legacies was complex.

71 *"Synthesis"* Accounting for species and site responses to drought provides a better
72 understanding of the magnitude and duration of drought legacies on forest growth and
73 productivity. Despite the widespread occurrence of growth reductions in the years during
74 and after drought occurrence, significant legacies were not very common, mostly lasted
75 one year and were more widespread in gymnosperms. These are relevant factors to be
76 considered in the future when studying the consequences of drought on forest
77 productivity and tree growth.
78
79
80 **Keywords:** dendroecology, drought intensity, global change ecology, growth variability,
81 NDVI, SPEI, tree rings.
82
83

## Introduction

Forests may be increasingly more stressed by droughts and warmer conditions (Babst *et al*. 2019) because more severe water shortage impairs the functioning of trees by reducing their photosynthesis and growth rates. Since drought constrains radial growth, the occurrence of dry spells results in the formation of narrow or missing growth rings that can be identified, cross-dated and measured (Schweingruber 1986; Fritts 2001). Thus, relating historical droughts to tree-ring widths allows to quantify the response of forests to drought and to forecast their vulnerability to future extreme climate events (Camarero *et al.* 2015a; Sánchez-Salguero *et al.* 2017). Previous studies demonstrated that the negative impacts of droughts on growth produced legacies which can last for several years (Becker 1989; Orwig & Abrams 1997). Recently, the interest in such long-term impacts of drought on forest growth has been reactivated (e.g. Anderegg *et al.* 2015; Huang *et al.* 2018; Peltier & Ogle 2019a, 2019b), opening questions on how drought triggers legacy effects which can mediate forest resilience capacity in sight of climate change (Camarero *et al.* 2018; Gao *et al.* 2018; Peltier & Ogle 2019b).

However, reconstructing forest resilience from tree growth patterns represents a limited, bottom-up approach, which can be complemented with the use of other ecosystem-level measures or proxies of forest productivity (Coulthard *et al.* 2017; Zhang *et al.* 2017; Gazol *et al.* 2018). Dendrochronological studies generally consider dominant trees in harsh sites to reduce the influence of tree to tree interactions in the stand and maximize the climate signal (Fritts 2001). Thus, when these measures at the individual tree level are upscaled to stand and forest levels there is a potential bias in the quantification of growth and productivity responses to drought due to the increase in uncertainty (Nehrbass-Ahles *et al.* 2014; Zhang *et al.* 2017). In this respect, satellite-based estimations of vegetation indices such as the Normalized Difference Vegetation

Index (NDVI), which is available since the early 1980s (Tucker 1979), can complement our understanding on the consequences of droughts on forest resilience (Vicente-Serrano *et al.* 2013; Zhang *et al.* 2017). The NDVI is mainly driven by changes in canopy greenness, tree cover and photosynthesis rate and thus it represents a quantification of gross primary production which complements radial growth (Vicente-Serrano *et al.* 2020). Thus, NDVI and tree-ring width data provide complementary estimations of forest productivity and growth that might be temporally decoupled due to their dependence on primary and secondary growth, respectively (Kannenberg *et al.* 2019a).

Forest growth resilience capacity to drought varies across biomes and continents (Gazol *et al.* 2017, 2018) due to phylogeny (angiosperms vs. gymnosperms), functional traits of tree species (e.g., wood density, wood anatomy, leaf features, etc.), and local adaptations (Anderegg *et al.* 2015; Peltier *et al.* 2016, 2017; Greenwood *et al.* 2017; Sánchez-Salguero *et al.* 2018; Kannenberg *et al.* 2019b). Anderegg *et al.* (2015) found more prevalent drought legacies in gymnosperms when considering tree growth responses to drought worldwide. Peltier *et al.* (2016) found that post-drought recovery times vary considerably within gymnosperms in dry forests from southwestern North America. Wider rings and higher autocorrelation (growth persistence) usually correspond to mesic sites dominated by angiosperms (Douglass 1941), whereas gymnosperms tend to present higher growth variability and abrupt growth reductions because of severe droughts (Anderegg *et al.* 2015). Thus, growth features such as year-to-year variability and autocorrelation can provide new insights on drought legacy effects.

However, the impact of drought on tree growth, and its legacy effects, can be influenced by external forcings mainly related to site characteristics and climate conditions (D'Orangeville *et al.* 2018; Kannenberg *et al.* 2019b). Pasho *et al.* (2011) found that the impact of drought on radial growth varied across species and sites in NE

Spain with species from xeric sites responding to drought at larger scales than species from mesic sites which mainly responded to short-duration, summer droughts. This different response suggests that site characteristics are important factors determining growth responses to drought, but also indicates that some tree species could be more vulnerable than others to certain drought types (D'Orangeville *et al.* 2018). For instance, Peltier & Ogle (2019a) speculated on the influence of physiological traits such as the mobility or storage of non-structural carbohydrates as an important factor modulating the response of tree species to drought. Regarding drought legacies, recent studies found that drought timing and duration modify the fate and duration of the legacy effects of drought on tree growth (Gao *et al.* 2018; Huang *et al.* 2018; Peltier & Ogle 2019a). Similarly, post-drought climate conditions can determine the duration of legacy effects (Jiang *et al.* 2019). All these results suggest that pre- and post-drought climate conditions need to be considered when quantifying drought legacies that can vary between tree species and as a function of site characteristics and climate conditions.

In this study, we take advantage of an extensive network of tree-ring width records (including 16,935 ring-width series of 16 tree species across 576 forests), and high-resolution climate and NDVI datasets to evaluate the strength and duration of the legacy effects of drought on tree growth and forest productivity. Moreover, we evaluate whether drought timing and intensity as well as tree growth features modulate these legacy effects. In particular we expect that: (i) drought legacy effects will be stronger in the case of radial growth than in the case of NDVI, (ii) growth legacies will differ among tree species, specifically gymnosperms will show longer legacies than angiosperms; and (iii) legacies will depend on growth variability (plasticity) and autocorrelation (persistence). We argue that this modulation will be influenced by how growth variability and autocorrelation vary along climate gradients and between species.

## Materials and methods

*Study area and tree growth data*

We studied forest growth in peninsular Spain and the Balearic Islands in south-western Europe (**Fig. S1**). We used a recently created database of tree-ring width measures from 576 forests of 16 tree species (9 gymnosperms and 7 angiosperms) across their Spanish distribution (**Table 1;** Gazol *et al.* 2018; Vicente-Serrano *et al.* 2020). We compiled raw tree-ring width information following dendrochronological methods (Fritts 2001) for 16,935 ring-width series. All wood samples were visually cross-dated, their annual rings were measured to a 0.01 mm resolution, and then these measurements were statistically checked to confirm the visual cross-dating (see more details in Gazol *et al.* 2018). The database contains growth information on the most widely distributed tree species across Spain (**Fig. S1**). The climate in the Iberian Peninsula differs between the humid north and north-west regions and the semi-arid south-east regions (De Castro *et al.* 2005). In northern Spain, the climate is temperate and presents high precipitation in winter (Martín-Vide & Olcina 2001). The transitional areas between central and north Spain present humid and continental Mediterranean conditions characterized by cold winters and dry summers, whereas the southeast areas have a semiarid and Mediterranean climate with a rainfall maximum in autumn (Martín-Vide & Olcina 2001). The overall average annual temperature of Spain ranges between 6° C near the alpine treeline in the Pyrenees (ca. 2,300 m a.s.l.) to ca. 19° C in the south and semiarid south-eastern regions. Similarly, total annual rainfall ranges between ca. 2,100 mm at the most humid sites to 250-350 mm in the driest areas (Martín-Vide & Olcina 2001). Mountain ranges modify the local temperature and precipitation regimes and enhance the local environmental heterogeneity.

184

185 *Climate and NDVI data*

186 Climatic data were obtained from a ~1.1 km$^2$-gridded and homogenized database of
187 climate records in the continental Spain and Balearic Islands derived from the entire
188 observational climatic data bank of the Spanish Meteorological Agency (AEMET) for the
189 period 1962−2008 (Vicente-Serrano *et al.* 2017). The dataset contained records of weekly
190 mean temperature, relative humidity, wind speed and totals for sunshine duration (as a
191 surrogate of the solar radiation) and precipitation. Evapotranspiration was calculated
192 using the FAO-56 Penman-Monteith Equation (Allen *et al.* 1998). We also calculated a
193 drought index, the Standardized Precipitation-Evapotranspiration Index (SPEI; Vicente-
194 Serrano *et al.* 2010), to quantify the spatial and temporal differences in drought severity.
195 Negative/positive SPEI values indicate dry/moist conditions. A detailed explanation of
196 the climate data processing and grid validation can be found in Vicente-Serrano *et al.*
197 (2017). To evaluate the time and duration at when drought most affected growth, we
198 calculated 1-, 3-. 6-, 9-, 12-, 15 and 18-month SPEI values for February, May and August
199 over the period 1982−2008.

200 To quantify the temporal variability in forest productivity, we used bi-weekly
201 time series of NDVI over the period 1982–2008 using a high resolution (1.1-km grid)
202 dataset obtained using the entire available daily NOAA–AVHRR images covering the
203 study period (see more details in Martín-Hernández *et al.* 2017).

204

205 **Table 1.** Studied tree species and data of radial growth. For each species, the number of
206 sites and trees together with the mean tree-ring width and its standard deviation (SD) are
207 shown for the period 1980−2008.

| Group | Species (code) | Nº. sites (Nº trees) | Tree-ring width | SD (mm) |
|---|---|---|---|---|

| | | | (mm) | |
|---|---|---|---|---|
| Gymnosperms | *Abies alba* (ABAL) | 48 (760) | 2.25 | 0.91 |
| | *Abies pinsapo* (ABPN) | 13 (223) | 1.65 | 0.73 |
| | *Juniperus thurifera* (JUTH) | 16 (242) | 1.28 | 0.64 |
| | *Pinus halepensis* (PIHA) | 116 (1710) | 1.90 | 1.06 |
| | *Pinus nigra* (PINI) | 67 (1214) | 1.16 | 0.58 |
| | *Pinus pinaster* (PIPI) | 18 (375) | 2.25 | 1.20 |
| | *Pinus pinea* (PIPN) | 9 (203) | 1.49 | 0.87 |
| | *Pinus sylvestris* (PISY) | 73 (1194) | 1.65 | 0.76 |
| | *Pinus uncinata* (PIUN) | 36 (575) | 0.92 | 0.32 |
| Angiosperms | *Castanea sativa* (CASA) | 10 (205) | 2.47 | 1.06 |
| | *Fagus sylvatica* (FASY) | 51 (681) | 1.63 | 0.65 |
| | *Quercus faginea* (QUFA) | 19 (295) | 1.38 | 0.67 |
| | *Quercus ilex* (QUIL) | 15 (57) | 1.16 | 0.66 |
| | *Quercus petraea* (QUPE) | 7 (123) | 1.54 | 0.57 |
| | *Quercus pyrenaica* (QUPY) | 34 (439) | 1.55 | 0.71 |
| | *Quercus robur* (QURO) | 35 (518) | 1.68 | 0.68 |

*NDVI drought legacies and tree-ring methods*

Generalized Additive Models (Wood 2017) were used to quantify drought legacies in NDVI for the period 1982−2008. We modeled how NDVI varied along that period using a cyclic cubic regression spline to capture intra-annual variations and a thin plate regression spline to represent long-term NDVI trends (**Fig. S2**). These analyses were performed using the "*mgcv*" library in R (Wood 2017). This allowed calculating the expected intra-annual variation and trend in NDVI and comparing it with observed NDVI values. Differences between observed and modelled values (i.e. residuals) may represent the effect of climate variations. Thus, we calculated bi-weekly residual variations in NDVI values as the difference between observed ($NDVI_{OBS}$) and predicted NDVI values

219 ($NDVI_{PRE}$). These bi-weekly residuals were averaged over a year to obtain standardized
220 and detrended NDVI series ($NDVI_{STD}$). Finally, autoregressive modeling was performed
221 to remove AR(n) (i.e. the dependency of NDVI in year *t* from NDVI in year *t*-n) thus
222 obtaining pre-whitened or residual NDVI series ($NDVI_{RES}$). These analyses were
223 performed using the "*dplR*" library in R (Bunn *et al.* 2018).

224 To obtain mean series of RWI values or site chronologies, tree-ring width
225 measurements were detrended using standard dendrochronological protocols (Fritts
226 2001). Each individual TRW series was detrended with a cubic smoothing spline with a
227 50% frequency response cutoff at 30 years. After that, RWIs were obtained by dividing
228 the observed by the fitted TRW values. The individual standardized RWI series were
229 averaged into mean site chronologies using bi-weight robust means ($RWI_{STD}$). In
230 addition, we built pre-whitened residual ring width index chronologies ($RWI_{RES}$) in
231 which autoregressive modeling was performed to remove AR(n) (i.e. the dependency of
232 growth in year *t* from growth in year *t*-n). These analyses were performed using the
233 "*dplR*" library (Bunn *et al.* 2018).

234 We calculated the mean $RWI_{STD}$ and its standard deviation (SD) for each
235 individual chronology to quantify the variation in growth (hereafter $RWI_{SD}$) in the period
236 1980–2008. We also calculated the first-order temporal autocorrelation of each mean site
237 chronology ($RWI_{STD}$) in the period 1980–2008 (hereafter $RWI_{AR}$). The $RWI_{AR}$ is a
238 measure of growth persistence, i.e. it quantifies how similar are RWI values between
239 consecutive years (Fritts 2001). Since not all chronologies spanned the entire period, both
240 $RWI_{SD}$ and $RWI_{AR}$ were calculated for a common period across most chronologies
241 (1980–1999).

242 Drought legacies were calculated up to three years after drought following
243 Anderegg *et al.* (2015). First, we identified the time scale at which tree growth ($RWI_{RES}$)

responded most tightly to drought (SPEI). Second, a linear model was used to predict $RWI_{RES}$ and $NDVI_{RES}$ using the selected SPEI. Finally, drought legacies were calculated by subtracting the predicted values of $RWI_{RES}$ and $NDVI_{RES}$ from the detrended-only RWI ($RWI_{STD}$) and NDVI ($NDVI_{STD}$) series, respectively. Prior to the calculation of drought legacies, $RWI_{RES}$ and $NDVI_{RES}$ as well as $RWI_{RES}$ and $NDVI_{RES}$ were scaled to have a mean of exactly one.

We used Linear Mixed-effect Models (LMM; Pinheiro & Bates 2000) to determine the significant time scale at which drought (SPEI) impacted most pre-whitened residual ring width index chronologies ($RWI_{RES}$) for each species. Site identity was regarded as a random factor since multiple measures (different year) occurred in each site. We ran separate models for each SPEI variable and ranked all potential models according to their corrected Akaike information criterion (AICc, see Burnham & Anderson 2002). We selected as the best model that showing the lowest AICc value, and the largest Akaike weight ($w_i$), which represents the relative probability that the selected model is the best one. The SPEI selected in the best model was used to quantify RWI and NDVI legacies.

For each species and site, extreme drought events were identified as the 20% SPEI values at the selected scale for the period 1980–2008. Since we were interested in legacies of extreme droughts, we only focused in RWI and NDVI drought legacies after the occurrence of such extreme events. The number of extreme droughts can vary between sites since not all chronologies span the entire period (1980–2008). We allowed for the occurrence of consecutive extreme events (e.g. 1994 and 1995) and legacies were calculated for the two events.

*Statistical analyses*

Superposed Epoch Analysis (SEA) was used to test the probability that RWI and NDVI drought legacies differed from random (Haurwitz & Brier 1981; Lough & Fritts 1987; Rao et al. 2019). For each site, RWI and NDVI legacies up to three years immediately after each extreme drought were averaged. We tested whether legacies from one up to three years after extreme droughts (site-specific 20% SPEI values) significantly ($p < 0.05$) differed from random using bootstrap resampling. For this purpose, we used the SEA function developed by Rao et al. (2019) which allows normalizing the pre-drought event years (setting the pre-drought legacies to a mean of 0). We used the three years before the drought event to normalize the data in each window. Due to the variation in the length of the chronologies and the occurrence of drought events, these analyses were only possible in 508 out of the 576 studied sites.

Pearson correlation analyses were used to quantify the relationships between RWI and NDVI drought legacies from one up to three years. We used Generalized Least-Square models (GLS; Pinheiro & Bates 2000) to quantify the differences in growth persistence ($RWI_{AR}$) and growth variability ($RWI_{SD}$) between sites and species. Site differences were represented as differences in average climate and tree growth. Mean climate conditions were represented by calculating the annual climate water balance as the difference between precipitation and reference evapotranspiration (P–PET). Tree growth was represented by means of the averaged tree-ring width for the period 1980–1999. In addition, tree species (16 levels) was considered to account for differences between species. We also considered potential interactions between growth, water balance and tree species. Since the number of chronologies varies between species (see **Table 1**), we used a constant variance structure to allow different variances between species (Pinheiro & Bates 2000).

We also applied GLSs to evaluate the relationship between RWI and NDVI drought legacies, and to determine which factors influenced their variation. To evaluate the factors influencing the variation in RWI and NDVI, covariates were standardized subtracting the mean and dividing by the standard deviation prior to the analyses to obtain comparable parameters across covariates (Schielzeth 2010). For RWI and NDVI legacies up to three years after a drought, we built models in which the water balance, tree species identity and its interaction were used as covariates. In other words, we tested whether the site characteristics, in terms of water availability, modulated the relationship between drought legacies and tree species. For modeling RWI legacies, we also included $RWI_{SD}$ and $RWI_{AR}$ and their interaction with water balance and tree species. This was done to evaluate how growth features and its variation influence growth legacies after drought. We used a constant variance structure to allow different variances between species (Pinheiro & Bates 2000).

We applied a multi-model inference approach based on information theory (Burnham & Anderson 2002) to select the set of covariates that better explained growth persistence, growth variability and legacies. We ranked all potential models according to their AICc and selected as the best model that showing the lowest AICc value and the largest $w_i$. When models showed a difference in AICc < 2, we selected the model with the lowest number of covariates. The models were ranked according to the ΔAICc (AICc differences between the selected model and the rest of models). All statistical analyses were performed using the R free software environment (R Core Team 2018). The *gls* function of the "*nlme*" package was used to fit the GLSs (Pinheiro *et al.* 2014), and the "*MuMin*" package was used to perform the multi-model selection and to calculate $R^2$ (Barton 2012).

## Results

The selected droughts impacted more negatively RWI than NDVI (**Fig. 1; Fig. S3**). The studied species responded significantly to drought (SPEI) by reducing growth (RWI) and NDVI at least at one time scale (**Figs. S4, S5**). The timescale at which RWI and NDVI responded to drought varied across species. Despite extreme droughts varied across sites, these events were more common in years 1986, 1994, 1995, 1999 and 2005 (**Fig. 1**). Particularly, 1986, 1994 and 2005 were considered extreme droughts in more than 60% of the sites, whereas 1989, 1995 and 1999 were considered extreme droughts in 30-40% of the sites (**Fig. S6**). Lower values of RWI were coupled with drought, whereas lower values of NDVI were mainly decoupled from those drought events (**Fig. 1**).

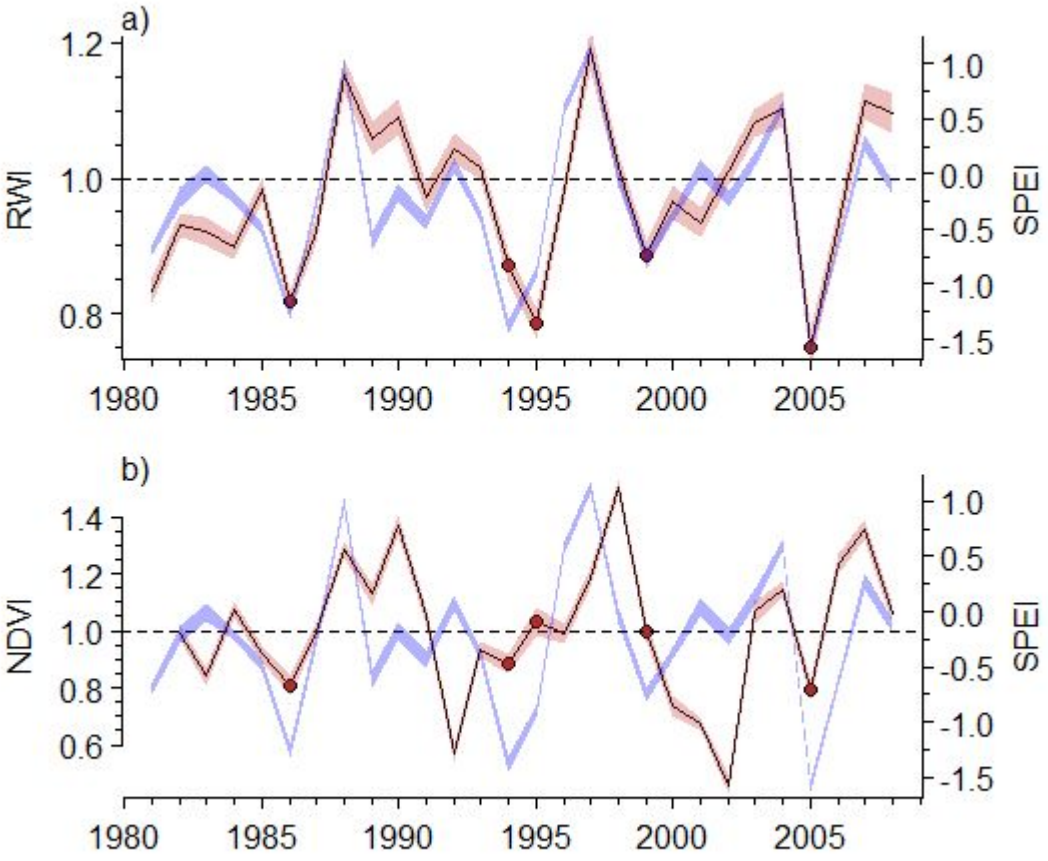

329 **Figure 1**. Tree growth (RWI, ring-width index), NDVI and their legacies for the period
330 1980–2008. (a) Average RWI across the study sites (red lines) and average SPEI values
331 (blue lines). In plot (b), average NDVI across the studied sites (red lines) and average
332 SPEI values (blue lines) are shown. The more common droughts across sites (1986, 1994,
333 1995, 1999, and 2005) are marked with red dots. Polygons indicate the standard error
334 (SE) of the mean.

335

336 **Table 2.** Percentage of sites displaying significant negative legacies in tree growth (RWI)
337 and NDVI from one (e.g. year 1) up to three (e.g. year 3) years after drought occurrence.
338 For each site, the significance of legacies ($p < 0.05$) was determined by means of
339 Superposed Epoch Analysis. Species codes are as in Table 1.

| | Growth legacies | | | NDVI legacies | | |
|---|---|---|---|---|---|---|
| Tree species (code) | *year 1* | *year 2* | *year 3* | *year 1* | *year 2* | *year 3* |
| *Abies alba* (ABAL) | 13.6 | 4.5 | 6.8 | 0.0 | 0.0 | 2.3 |
| *Abies pinsapo* (ABPN) | 8.3 | 8.3 | 0.0 | 0.0 | 16.7 | 0.0 |
| *Castanea sativa* (CASA) | 10.0 | 0.0 | 10.0 | 10.0 | 0.0 | 10.0 |
| *Fagus sylvatica* (FASY) | 18.8 | 6.3 | 4.2 | 0.0 | 2.1 | 2.1 |
| *Juniperus thurifera* (JUTH) | 13.3 | 13.3 | 0.0 | 0.0 | 0.0 | 0.0 |
| *Pinus halepensis* (PIHA) | 8.0 | 6.0 | 3.0 | 21.0 | 11.0 | 6.0 |
| *Pinus nigra* (PINI) | 10.2 | 1.7 | 0.0 | 0.0 | 5.1 | 3.4 |
| *Pinus pinaster* (PIPI) | 5.6 | 5.6 | 0.0 | 5.6 | 16.7 | 5.6 |
| *Pinus pinea* (PIPN) | 11.1 | 0.0 | 0.0 | 22.2 | 0.0 | 0.0 |
| *Pinus sylvestris* (PISY) | 8.2 | 8.2 | 1.6 | 0.0 | 8.2 | 9.8 |
| *Pinus uncinata* (PIUN) | 19.2 | 0.0 | 7.7 | 3.8 | 3.8 | 3.8 |
| *Quercus faginea* (QUFA) | 0.0 | 0.0 | 0.0 | 0.0 | 0.0 | 0.0 |

| | | | | | | |
|---|---|---|---|---|---|---|
| *Quercus ilex* (QUIL) | 14.3 | 7.1 | 7.1 | 0.0 | 0.0 | 0.0 |
| *Quercus petraea* (QUPE) | 0.0 | 20.0 | 20.0 | 0.0 | 0.0 | 0.0 |
| *Quercus pyrenaica* (QUPY) | 0.0 | 6.3 | 3.1 | 0.0 | 0.0 | 3.1 |
| *Quercus robur* (QURO) | 3.4 | 3.4 | 17.2 | 0.0 | 13.8 | 20.7 |

340

341 Tree growth variability ($RWI_{SD}$) varied across species ($F = 41.66$; $p < 0.05$) but
342 also as a function of site annual water balance ($F = 36.72$; $p < 0.05$) and the mean tree
343 ring width ($F = 28.04$; $p < 0.05$). $RWI_{SD}$ was lower for trees forming wider rings ($\beta = -0.015 \pm 0.004$; $p < 0.05$). In addition, a significant interaction between tree species and
344 water balance was found ($F = 5.59$; $p < 0.05$) with the two species from the driest sites
345 (i.e. *P. pinea* and *P. halepensis*) showing a more steep slope relationship between water
346 balance and $RWI_{SD}$ than the rest of species (**Fig. 2**). The regression model accounted for
347 69% of the variation in $RWI_{SD}$. The growth persistence ($RWI_{AR}$) was the highest in *Q.*
348 *pyrenaica* and lowest in *P. uncinata*, with strong variation across species ($F = 7.65$; $p <$
349 0.05). We also found a significant influence of water balance on $RWI_{AR}$ ($F = 6.13$; $p <$
350 0.05) indicating that growth persistence was higher in dry places ($\beta = -0.07 \pm 0.03$; $p <$
351 0.05). However, we found no significant interactions between tree species and mean
352 annual water balance. The model accounted for 23% of the variation in $RWI_{AR}$.
353
354

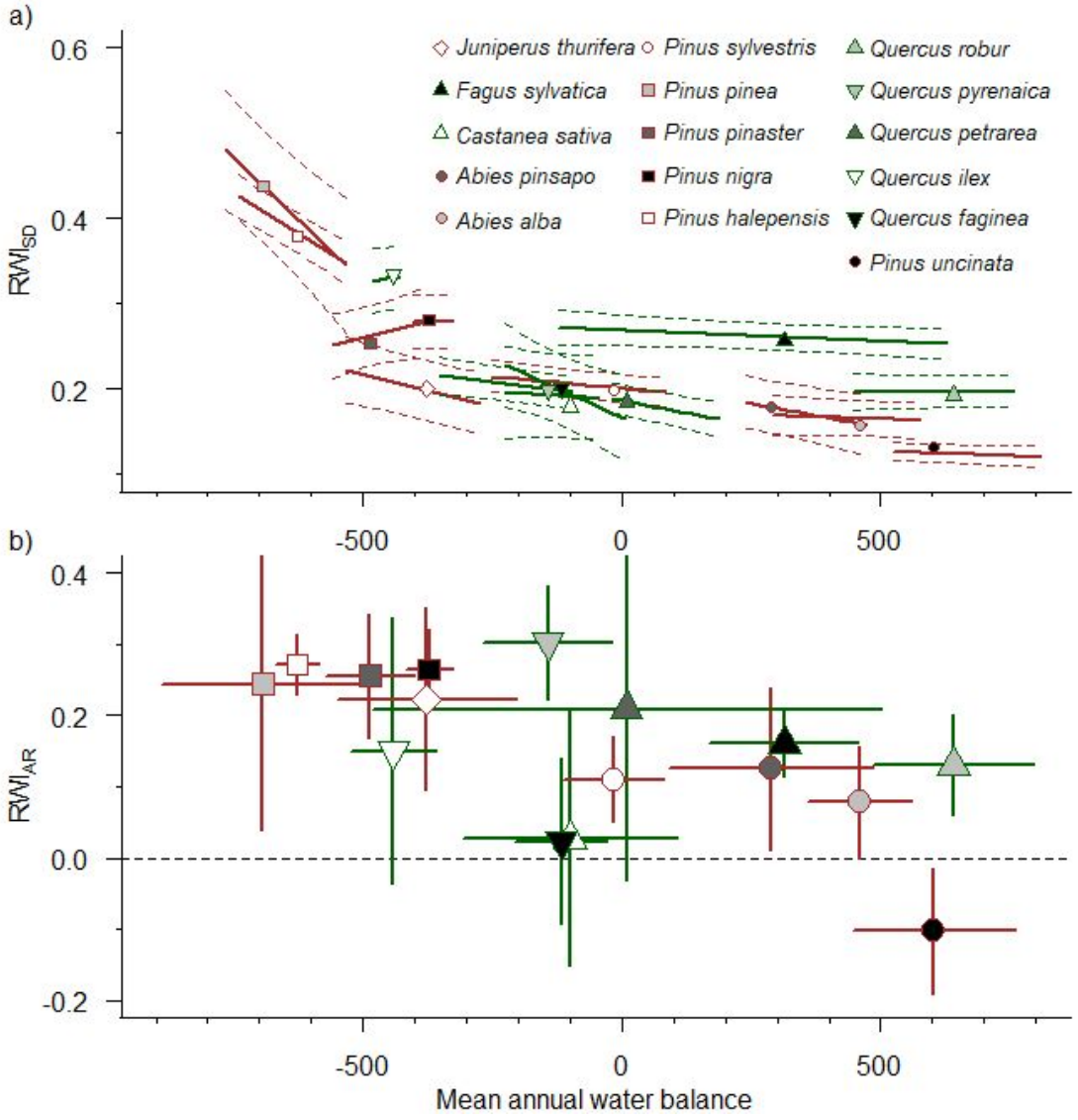


**Figure 2.** Variation in tree growth (a, $RWI_{SD}$) and growth persistence quantified as first-order autocorrelation (b, $RWI_{AR}$) across tree species and as a function of the mean annual water balance (P–PET, in mm). For each species, the point represents the average values across the forests where the species is present. In plot (a) solid lines represents regression slopes (dashed lines are 95% confidence intervals) for the interaction between water balance and tree species. In plot (b) the horizontal and vertical segments are the 95% confidence intervals of the water balance and the $RWI_{AR}$, respectively. Green colors indicate angiosperms and red colors are gymnosperms.

365 Drought legacies on RWI and NDVI (i.e. the difference between detrended-only
366 and predicted pre-whitened series) varied between species (**Figs. 3** and **4**; **Tables 2** and
367 **S1**). RWI and NDVI drought legacies were only significantly correlated in the first year
368 after drought ($r = 0.11$; $p = 0.02$). First-, second- and third-year RWI legacies were
369 positively related (**Table S2**). First-year RWI legacies were mostly negative (341 sites,
370 67% of sites) despite only significant in 9.4% of the forests studied (i.e. 48 sites; see
371 **Table 2**). Second- and also third-year RWI legacies were negative in 51.1% and 43.9% of
372 the studied sites (**Table S1**), but significant only in 5.1% and 4.4% of them, respectively.
373 First- and second-year RWI legacies were negative in 215 sites (being only significant in
374 9 sites), and 3-year consecutive negative legacies were observed in 143 sites (only
375 significant in 1 sites). First-, second- and third-year NDVI legacies were positively
376 related (**Table S2**). First-year NDVI legacies varied between species, they were negative
377 in 50.7% of sites, but they were only significant in 5.1% of them (**Figs. 3** and **4**; **Tables 2**
378 and **S1**). Second- and also third-year NDVI legacies were mostly negative (53.1% and
379 51.1% of sites, respectively) and significant in 5.9% and 5.1% of the studied sites,
380 respectively. First- and second-year NDVI legacies were negative in 199 sites (only
381 significant in 9 sites with 8 *P. halepensis* forests among them), and 3-year consecutive
382 negative legacies were observed in 154 sites (only significant in 2 sites).
383

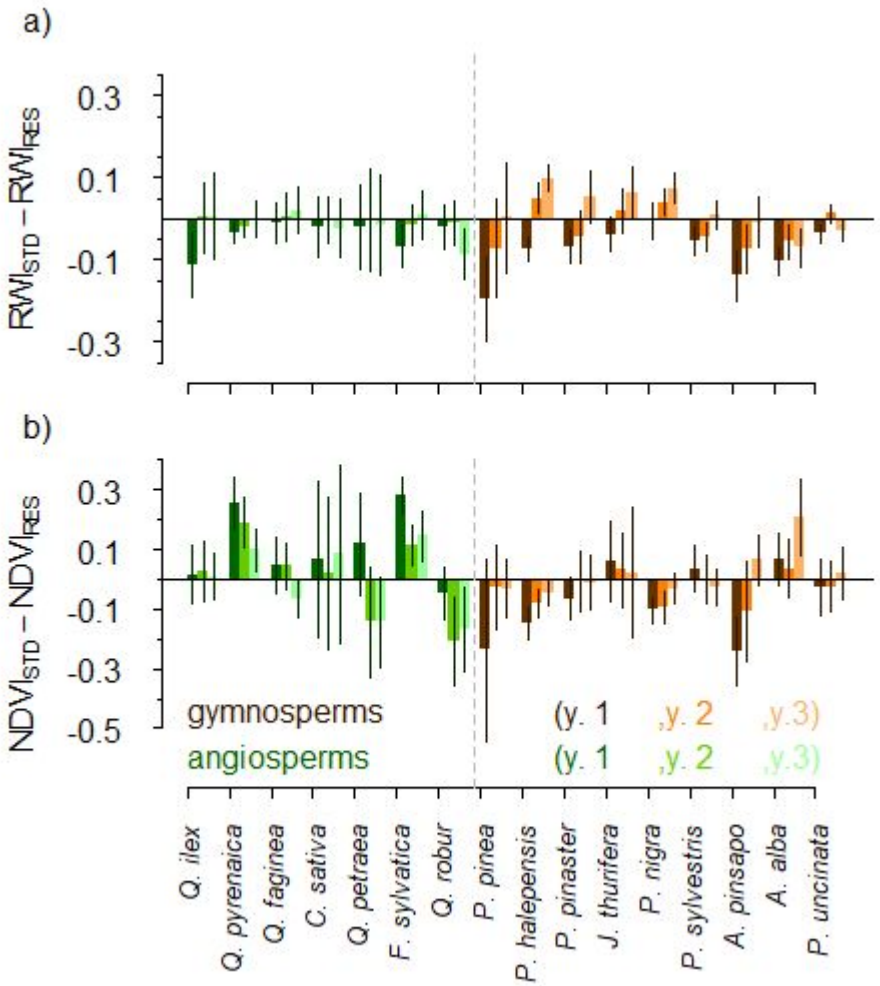


**Figure 3.** Post-drought legacies of tree species calculated for one (y.1), two (y.2) and three (y.3) years. Legacies were calculated for tree growth variability (RWI, a) and NDVI (b) as: (a) the difference between standard ($RWI_{STD}$) and residual ($RWI_{RES}$) ring-width indices, and (b) the difference between standard ($NDVI_{STD}$) and residual ($NDVI_{RES}$) NDVI data. Angiosperms and gymnosperms are represented in green and brown-orange colors, respectively. Colour intensity indicates the years after drought. The vertical segments represent the 95% confidence intervals for the mean, and the vertical dashed grey line separates angiosperms and gymnosperms.

First-year RWI legacies depended on tree species identity and growth variability ($RWI_{SD}$), and also on their interaction (**Figs. 3** and **4**; **Table 3**). The selected model

396 accounted for 30% of the variation in the data (**Tables 3** and **S3**). More negative legacies
397 during the first year were observed in conifers (**Fig. 3**). The relationship between first-
398 year legacies and growth variability ($RWI_{SD}$) varied considerably across species but
399 without a clear pattern (**Fig. 4**). Second-year RWI legacies were dependent on tree
400 species identity, $RWI_{SD}$, and the interaction between them (**Table 3**; **Fig. S7**). The model
401 accounted for 30% of the variation in the data. Second-year RWI legacies tended to be
402 negative in trees with relatively variable growth from mesic sites (**Fig. 3**). Finally, third-
403 year legacies depended on the same variables as the first- and second-year legacies
404 (**Table 3**; **Fig. S8**), and the model explained 34% of the variation in the data.
405 NDVI legacies depended on the water balance, varied across species and with the
406 interaction of these variables (**Table 3**; **Fig. 3**). First-year NDVI legacies depended on the
407 interaction between tree species and water balance (**Fig. 4**). The selected model
408 accounted for 39% of the variation in the data (**Tables 3** and **S4**). The model for the
409 second-year NDVI legacies explained 22% of the variation in the data and included tree
410 species identity and water balance as covariates (**Table 3**). NDVI legacies increased in
411 wet sites ($\beta = -0.05 \pm 0.02$; $p < 0.05$; **Fig. S9**). The model of third-year NDVI legacies
412 explained 39% of its variation, and included as covariates tree species identity, water
413 balance and their interaction (**Table 3**; **Fig. S10**).

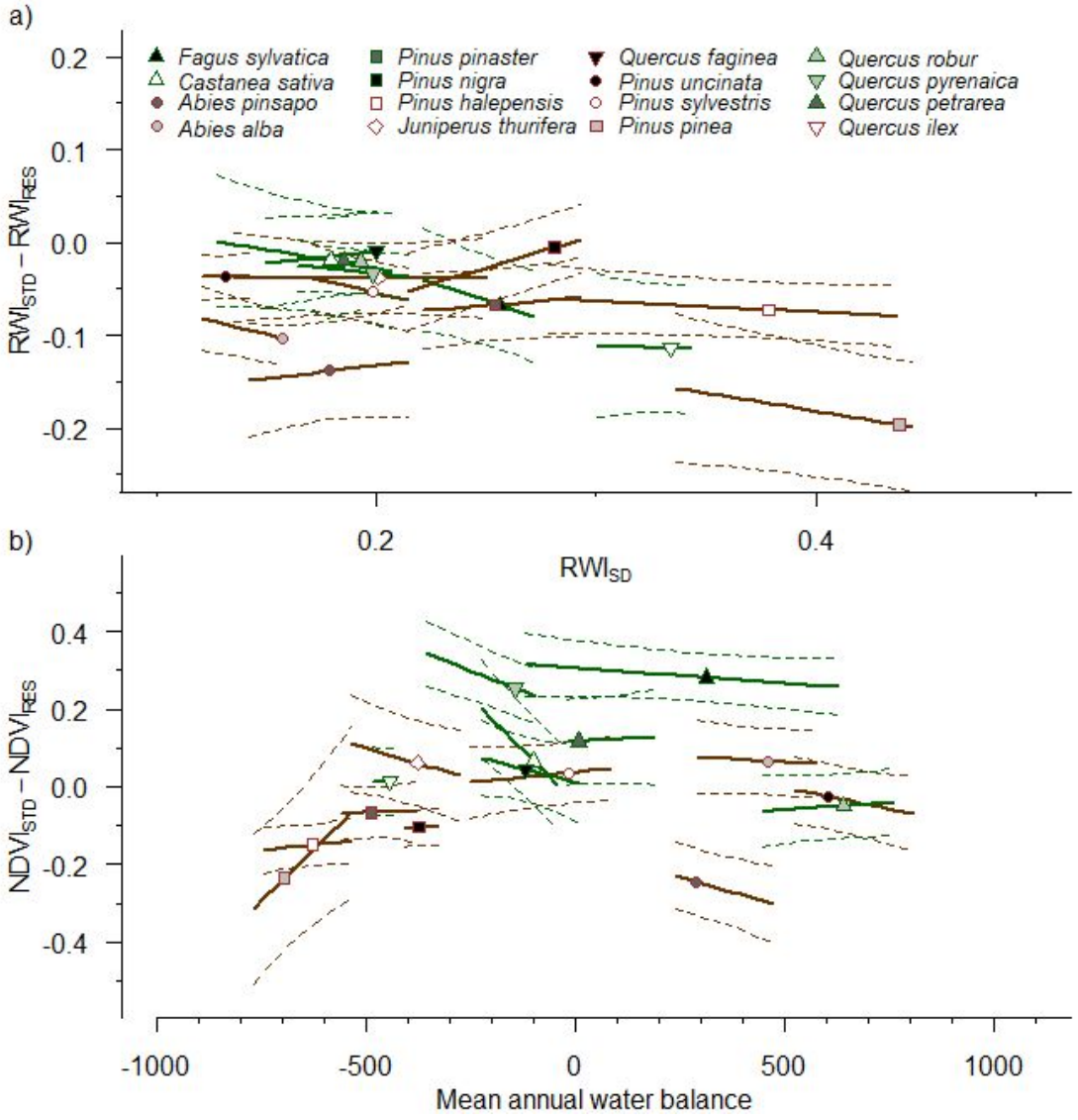


**Figure 4.** Variation of (a) post-drought growth legacies ($RWI_{STD}$ –$RWI_{RES}$) in the first year after drought between species and according to growth variability ($RWI_{SD}$); and (b) post-drought NDVI legacies ($NDVI_{STD}$ –$NDVI_{RES}$) in the first year after drought between species and according to mean annual water balance (P–PET, in mm). For each species, the line represents the regression slope for the relationship between the explanatory variable and first-year legacies and the dashed segments are the 95% confidence intervals of the prediction. Species are ordered according to the water balance of the regions they inhabit from dry-warm sites (e.g. *P. pinea*) to wet-cool sites (e.g. *Q. robur*).

424 **Table 3.** Selected generalized least square models characterizing the variation in growth
425 (RWI) and NDVI legacies from one up to three years after drought. For each variable, the
426 *F* statistic and the associated probability (* $p < 0.05$; ** $p < 0.01$) are shown.
427 Abbreviations: P–PET, water balance; $RWI_{AR}$, ring-width index first-order
428 autocorrelation (persistence); $RWI_{SD}$, standard deviation of the ring-width index (growth
429 variability); AICc, second-order Akaike information criterion; $R^2$ proportion of explained
430 variance.

| | Tree species | P–PET | $RWI_{SD}$ | Tree species * $RWI_{SD}$ | Tree species * P–PET | AICc | $R^2$ |
|---|---|---|---|---|---|---|---|
| Growth | | | | | | | |
| *year 1* | 4.42** | – | 2.08 | 4.15** | | 1.90 | 0.30 |
| *year 2* | 3.22** | | 0.01 | 3.32** | | 0.80 | 0.30 |
| *year 3* | 6.67** | | 1.30 | 6.88** | | 0.78 | 0.34 |
| NDVI | | | | | | | |
| *year 1* | 15.62** | 9.43** | | | 3.83** | 9.48 | 0.39 |
| *year 2* | 4.95** | 7.95** | | | | 5.09 | 0.22 |
| *year 3* | 4.56** | 39.74** | | | 3.12** | 3.87 | 0.39 |

## Discussion

Lower than expected radial growth rates in the years following an extreme drought event are widespread in Spanish forests, particularly in the first year after drought occurrence. However, these drought legacies are significantly different from random in only 9% of forests. This seldom occurrence of significant drought legacies was drastically reduced in the second and third years after drought occurrence with only 1 site showing significant legacies in three consecutive years. This suggests that the drought effects mainly occurred in the first year after drought. Nevertheless, our results also indicate that differences between species in legacies reflect complex response patterns across broad biogeographical gradients (D'Orangeville *et al.* 2018), with more intense legacies occurring in dry regions where tree-growth variability is high. The legacies of drought on NDVI also varied between species and sites but were poorly correlated with RWI legacies and the selected droughts suggesting that canopy greenness and growth responses are decoupled (Stocker *et al.* 2019; Kannenberg *et al.* 2019a). Non-significant NDVI legacies were also the rule rather than the exception and prevailed in conifers from dry sites (e.g. *P. halepensis*). Our results concur with previous studies highlighting the importance of drought on explaining growth variability and inducing growth legacies (Anderegg et al. 2015; Gao *et al.* 2018; Peltier & Ogle 2019b). Responses of tree species radial growth to drought varied considerably between tree species pointing to the necessity to account for drought timing and duration when studying growth responses across large scales (Pasho et al. 2011; Gao et al. 2018). Furthermore, our results evidence that accounting for growth variability substantially improves the understanding of drought growth legacies in forests. However, we failed to establish a link between growth persistence and drought legacies.

456 Growth legacies varied in magnitude between species and sites, and significant
457 first-year legacies were more common in gymnosperms (conifers) than in angiosperms
458 (broadleaved species) (**Table 2**). Several reasons mainly related with the selection of the
459 extreme drought events can explain the seldom occurrence of significant legacies. SEA
460 relies on bootstrapping to randomly select sets of the time series and to determine if
461 legacies for event years differ from random (Haurwitz & Brier 1981). Thus, the a priori
462 subjective definition of what constitutes an extreme drought can influence the ability to
463 detect significant legacies (Rao *et al*. 2019). We chose drought events with the
464 assumption that each species can vary in their response to drought in terms of when it
465 occurs (season) and how much it lasts (time scale). In line with previous studies, we
466 found that tree species from xeric sites responded more strongly to droughts at scales
467 from 12 to 15 months, whereas species from mesic sites were more impacted by short-
468 term droughts (Pasho *et al*. 2011). However, when selecting the extreme droughts (i.e.
469 the 20% lowest SPEI values) for each species and site, extreme droughts were very
470 similar and corresponded to previously detected severe events for their extensive impact
471 (Vicente-Serrano *et al.* 2014; Gazol *et al.* 2018). It might happen that an event not
472 included in the 20th SPEI lowest percentile can cause a marked growth reduction as
473 responses of radial growth to drought can be non-linear (Orwig & Abrams 1997). Along
474 this, low SPEI values can have reduced effects on growth if local microclimate or site
475 conditions mitigate drought impact (Jiang *et al*. 2019). Further, other confounding
476 factors besides drought can cause abrupt growth reductions as is the case of pest
477 outbreaks or pathogens (e.g. Sangüesa-Barreda *et al.* 2015). These factors can also
478 explain the occurrence of significant legacies in the second- or third- year after drought
479 occurrence despite no significant legacies were observed in the first-year. Further
480 research over longer periods of time and with different thresholds of drought occurrence

481 is required to fully determine whether significant legacies are more prevalent than
482 observed here.

483 Regarding their magnitude, we found stronger growth reductions and more
484 marked legacy effects in gymnosperms than in angiosperms (Anderegg *et al.* 2015;
485 Peltier *et al.* 2016, 2017; Gazol *et al.* 2018; Huang *et al.* 2018). Legacy effects on tree
486 growth one year after drought were negative in Mediterranean pine species from dry
487 regions. Particularly, *P. pinea* and *P. halepensis* displayed more marked legacies during
488 the first year after drought than other gymnosperms from wetter areas. However, these
489 species, particularly *P. halepensis*, were able to recover growth in the second and third
490 years. These results indicate that gymnosperms from dry areas have a great capacity
491 (resilience) to recover after drought (Gazol *et al.* 2018; Sánchez-Salguero *et al.* 2018).
492 This can be explained because Mediterranean conifers may present a bimodal
493 xylogenesis (e.g. Camarero *et al.* 2010; Pacheco *et al.* 2018), which has also been
494 observed in evergreen Mediterranean oaks (Gutierrez *et al.* 2011), and can explain the
495 large difference between first- and second year drought legacies these oak species as *Q.*
496 *ilex*. This behaviour allows trees to grow during the spring and autumn seasons with
497 favourable (wet, cool) climate conditions, which facilitates a fast growth recovery once
498 trees are released from summer drought stress. This will explain why there is a high
499 proportion of sites with significant first-year legacies in *P. halepensis*, *J. thurifera* and
500 *Q. ilex* despite the occurrence of second-year negative legacies is less frequent. In other
501 gymnosperms inhabiting colder sites, growth is mainly unimodal, and it peaks in early
502 to mid-summer (Rossi *et al.* 2006), which makes these species less resilient to rare
503 summer droughts.

504 However, several gymnosperms from mesic and even cold sites also displayed
505 marked legacies in the year after drought occurrence. This is the case of *P. uncinata*, a

506 mountain pine species which growth is mainly limited by cold spring-summer
507 temperatures (Gutiérrez 1991; Camarero *et al.* 1998). Nevertheless, previous studies
508 have demonstrated that the growth of several *P. uncinata* populations included in this
509 study can be impacted by drought (Camarero *et al*. 2015b). Negative legacies of drought
510 in growth were evident in fir species (*A. alba* and *A. pinsapo*). The growth of *A. alba* is
511 highly dependent on summer conditions (Pasho *et al.* 2011), but it also depends on
512 previous-year, mid-term climate conditions including late-summer water deficit
513 (Linares *et al.* 2010; Camarero *et al.* 2011). Moreover, widespread drought-induced
514 growth decline of these species has been observed over the last decades which agrees
515 with the widespread occurrence of negative growth legacies.
516 Regarding angiosperms, legacies of drought were more evident in *F. sylvatica*
517 and *Q. ilex* than in the rest of species. Recently, it has been observed a warming-related
518 growth decline of European beech populations from Atlantic and Mediterranean regions
519 of northern Spain (Serra-Maluquer *et al*. 2019). Thus, in this warming context the
520 impacts of severe droughts can have consequences on growth in the year after its
521 occurrence. However, broadleaved species such as *C. sativa* and *Q. robur*, which grow
522 in mesic forests, and other oak species such as *Q. pyrenaica* showed no clear growth
523 legacies. In the case of *C. sativa* and *Q. robur* it is possible that drought intensity is low
524 in the mesic regions they inhabit, and they may be more sensitive to other climate
525 extremes (e.g., heat waves) than to droughts (Leuzinger *et al.* 2005). However, these
526 authors also highlighted the ability of *Q. robur* to cope with severe droughts, which may
527 explain the lack of legacies.
528 We found that growth variability ($RWI_{SD}$) affected drought legacies differently
529 depending on the species. However, we found no influence of growth persistence
530 ($RWI_{AR}$) on the legacies of drought on growth. Higher growth persistence is expected to

increase drought legacies (Peltier *et al.* 2017; Peltier & Ogle 2019b), but higher persistence would also be expected on mesic sites dominated by angiosperms (Fritts 2001). We found marked variations in growth persistence between species and a pattern towards increasing growth persistence in dry sites dominated by gymnosperms (conifers). Furthermore, the highest autocorrelation values were observed in pine species from dry regions. The lack of relationship between growth persistence and drought legacies can be explained by the predominantly short duration of drought legacies on growth.

Identifying how growth variability influences legacies is less straightforward. When growth variability is driven by inter-annual climate fluctuations, we can expect a larger legacy effect with the increase in growth variability, as can be expected in gymnosperms from dry regions whose growth is severely constrained by drought (Del Río *et al.* 2014; Gazol *et al.* 2018; Sánchez-Salguero *et al.* 2018). This is also supported by the negative relationship found between mean tree-ring width and growth variability. The variability in growth in pine species growing in semiarid areas such as *P. halepensis* can be the reason why those species present greater than expected growth two and three years after drought. Greater growth variability ($RWI_{SD}$) can also be expected in species from warm sites such as *Q. ilex* and the juniper *J. thurifera* which present a long growing season (Gutiérrez *et al.* 2011), than in species from cold mountain sites such as *P. uncinata* (Camarero *et al.* 1998). Growth variability can also vary at the intraspecific level particularly for those species that present wide geographical ranges in Europe and show plastic phenological responses such as *F. sylvatica*, *P. pinaster* and *P. sylvestris* (Sánchez-Salguero *et al.* 2018; Vilà-Cabrera & Jump 2019). The complex picture found in this study suggests that further studies

555 considering how growth variability and persistence influence legacies at the individual
556 level are clearly required.
557 NDVI legacies were less apparent than RWI legacies in agreement with the
558 lower responsiveness to water shortage of this variable as compared to RWI (see also
559 Gazol *et al.* 2018). Drought legacies in both growth and productivity were only slightly
560 related during the first year suggesting that these two components are to some degree
561 linked (e.g. Vicente-Serrano *et al.* 2013; Gazol *et al.* 2018; Vicente-Serrano *et al.* 2020).
562 On the one hand, these results agree with previous studies that found that the
563 relationship between radial growth and NDVI was high at annual scales (Vicente-
564 Serrano *et al.* 2020). On the other hand, primary and secondary growth may decouple
565 and respond to different climate processes acting at different spatial and temporal scales
566 (Kannenberg *et al.* 2019a). This can also lead to relations at different temporal scales
567 between RWI and NDVI across forests (Vicente-Serrano *et al.* 2020). Our results point
568 out in this direction and suggest that the timescale at which growth and NDVI respond
569 to drought varies depending on the species considered. Wood formation is a low-
570 priority component of growth representing stand-scale biomass accumulation as
571 compared with shoot and leaf growth which have a high priority as carbon sinks (Fritts
572 2001; Kannenberg *et al.* 2019a). Therefore, trees can allocate resources to primary
573 growth and photosynthetic activity in response to drought at a cost of reducing
574 secondary growth resulting in growth legacies. Furthermore, NDVI data was quantified
575 at a coarse scale indicating an ecosystem surrogate of forest productivity dependent on
576 canopy greenness and primary growth (Carlson & Ripley 1997). This, in turn may
577 dismiss the ability to detect the impact of drought on forest growth due to the presence
578 of different vegetation types. For instance, we found a marked persistence of NDVI
579 legacies in *P. halepensis* forests which are characterized by a fast growth recovery.

Discerning whether this occurs in pure and mixed stands or if it is affected by scale issues requires further studies using high-resolution satellite images. In addition, comparing pure and mixed forests dominated by different cover frequencies of gymnosperms and angiosperms are required to better understand the linkages between NDVI and tree-ring data.

We concur with previous studies on the importance of drought characteristics as drivers of growth responses to drought (Gao *et al.* 2018), but our results also suggest that drought legacies vary considerably in duration between species (Peltier *et al.* 2016). We have demonstrated here that growth variability is an important factor to be considered when explaining drought legacies, and that probably due to the short duration of most legacies they depend less than expected on growth persistence. In a previous study, we evaluated the resistance and recovery after drought of tree species in Spain and found a great resistance of broadleaved species from mesic regions and a great recovery capacity of conifers from dry regions (Gazol *et al.* 2018). Here we have refined our analyses by considering pre- and post-climate conditions when quantifying legacies of drought. The results partially confirm our previous findings suggesting that, if present, drought legacies will be more common in conifers inhabiting xeric regions which present a more variable growth. Along this, our results highlight the existence of variability in the strength and duration of drought legacies across tree species and point out further research by considering growth persistence and variability at the individual level.

**Acknowledgements**

This study was financially supported by: Xunta de Galicia, Grant/Award Number: PGIDIT06PXIB502262PR, GRC GI-1809; INIA, Grant/Award Number: RTA2006-

605 00117; CANOPEE, 2014-2020-FEDER funds; and Spanish Science Ministry: RTI2018-
606 096884-B-C31, RTI2018-096884-B-C33 and AGL2017-83828-C2-2R projects. GSB
607 was supported by a "Juan de la Cierva Formación" grant from MINECO (FJCI 2016-
608 30121). AG was supported by a project "2018 Leonardo Grant for Researchers and
609 Cultural Creators, BBVA Foundation". The foundation accepts no responsibility for the
610 opinions, statements and contents included in the project and/or the results thereof,
611 which are entirely the responsibility of the authors. Authors declare no conflict of
612 interest. We sincerely thank the in-depth analyses and comments provided by the
613 reviewers.

614

615 **Authors' contributions**

616 AG, JJC, RSS and SMV designed the study. All authors collected and processed the
617 data. AG, JJC and RSS analysed the data. AG and JJC drafted the manuscript and all
618 authors commented on it and contributed to its editing.

619

620 **Data availability**

621 Should the manuscript be accepted, the data supporting the results will be archived in
622 the Dryad public repository and the data DOI will be included at the end of the article.

623

624 **References**

625 Allen, R.G., Pereira, L.S., Raes, D. & Smith, M. (1998). *Crop evapotranspiration:*
626 *Guidelines for computing crop requirements*. Irrigation and Drainage Paper No. 56.
627 FAO, Rome,300 pp.

628 Anderegg, W.R.L., Schwalm, C., Biondi, F., Camarero, J.J., Koch, G., Litvak, M., et al.
629 (2015). Pervasive drought legacies in forest ecosystems and their implications for
630 carbon cycle models. Science, 349, 528–532.
631 Babst, F., Bouriaud, O., Poulter, B., Trouet, V., Girardin, M.P. & Frank, D.C. (2019).
632 Twentieth century redistribution in climatic drivers of global tree growth. Science
633 Advances, 5, eaat4313. doi: 10.1126/sciadv.aat4313.
634 Barton, K. (2012). MuMIn: Multi-model inference. R package version 1.7.7. Retrieved
635 from http://CRAN.R-project.org/package=MuMIn.
636 Becker, M. (1989). The role of climate on present and past vitality of silver fir forests in
637 the Vosges mountains of northeastern France. Can. J. For. Res., 19, 1110-1117.
638 Bunn, A., Korpela, M., Biondi, F., Campelo, F., Merian, P. & Qeadan, F., et al. (2018).
639 dplR: Dendrochronology Program Library in R. R package version 1.6.9.
640 https://CRAN.R-project.org/package=dplR
641 Burnham, K.P. & Anderson, D.R. (2002). *Model selection and multimodel inference: A*
642 *practical information-theoretic approach*. Springer-Verlag, NY, USA, 488 pp.
643 Camarero, J.J., Guerrero-Campo, J. & Gutiérrez, E. (1998). Tree-ring structure and
644 growth of *Pinus uncinata* Ram. and *Pinus sylvestris* L. in the Central Spanish
645 Pyrenees. Arct. Alp. Res., 30, 1–10.
646 Camarero, J.J., Olano, J.M. & Parras A. (2010). Plastic bimodal xylogenesis in conifers
647 from continental Mediterranean climates. New Phytol., 185, 471–480.
648 Camarero, J.J., Bigler, C., Linares, J.C. & Gil-Pelegrín, E. (2011). Synergistic effects of
649 past historical logging and drought on the decline of Pyrenean silver fir forests. For.
650 Ecol. Manage., 262, 759–769.

651 Camarero, J.J., Gazol, A., Sangüesa-Barreda, G., Oliva, J. & Vicente-Serrano, S.M.
652 (2015a). To die or not to die: Early warnings of tree dieback in response to a severe
653 drought. J. Ecol., 103, 44–57.
654 Camarero, J.J., Gazol, A., Galván, J.D., Sangüesa-Barreda, G. and Gutiérrez, E.
655 (2015b), Disparate effects of global-change drivers on mountain conifer forests:
656 warming-induced growth enhancement in young trees vs. $CO_2$ fertilization in old
657 trees from wet sites. Glob. Change Biol., 21, 738–749.
658 Camarero, J.J., Gazol, A., Sangüesa-Barreda, G., Cantero, A., Sánchez-Salguero, R.,
659 Sánchez-Miranda, A., et al. (2018). Forest growth responses to drought at short-
660 and long-term scales in Spain: squeezing the stress memory from tree rings. Front.
661 Ecol. Evol., 6, doi: 10.3389/fevo.2018.00009.
662 Carlson, T.N. & Ripley, D.A. (1997). On the relation between NDVI, fractional
663 vegetation cover, and leaf area index. Remote Sens. Env., 62, 241–252.
664 Coulthard, B.L., Touchan, R., Anchukaitis, K.J., Meko, D.M. & Sivrikaya, F. (2017).
665 Tree growth and vegetation activity at the ecosystem-scale in the eastern
666 Mediterranean. Environ. Res. Lett., 12, 084008. doi: 10.1088/1748-9326/aa7b26.
667 D'Orangeville, L., Maxwell, J., Kneeshaw, D., Pederson, N., Duchesne, L., Logan, T.,
668 et al. (2018). Drought timing and local climate determine the sensitivity of eastern
669 temperate forests to drought. Glob. Chang. Biol., 24, 2339–2351.
670 De Castro, M., Martín-Vide, J. & Alonso, S. (2005). *El clima de España: pasado,*
671 *presente y escenarios de clima para el siglo XXI. Impactos del cambio climático en*
672 *España*. Ministerio Medio Ambiente, Madrid, 64 pp.
673 Del Río, M., Rodríguez-Alonso, J., Bravo-Oviedo, A., Ruíz-Peinado, R., Cañellas, I. &
674 Gutiérrez, E. (2014). Aleppo pine vulnerability to climate stress is independent of
675 site productivity of forest stands in southeastern Spain. Trees, 28, 1209-1224.

676 Douglass, A.E. (1941). Crossdating in dendrochronology. J. For., 39, 825–831.
677 Fritts, H.C. (2001). Tree Rings and Climate. Balckburn Press, Caldwell, USA, 567 pp.
678 Gao, S., Liu, R., Zhou, T., Fang, W., Yi, C., Lu, R., et al. (2018). Dynamic responses of
679 tree-ring growth to multiple dimensions of drought. Glob. Chang. Biol., 24, 5380–
680 5390.
681 Gazol, A., Camarero, J.J., Anderegg, W.R.L. & Vicente-Serrano, S.M. (2017). Impacts
682 of droughts on the growth resilience of Northern Hemisphere forests. Glob. Ecol.
683 Biogeogr., 26, 166–176.
684 Gazol, A., Camarero, J.J., Vicente-Serrano, S.M., Sánchez-Salguero, R., Gutiérrez, E.,
685 de Luis, M., et al. (2018). Forest resilience to drought varies across biomes. Glob.
686 Chang. Biol., 24, 2143–2158.
687 Greenwood, S., Ruiz-Benito, P., Martínez-Vilalta, J., Lloret, F., Kitzberger, T., Allen,
688 C.D., et al. (2017). Tree mortality across biomes is promoted by drought intensity,
689 lower wood density and higher specific leaf area. Ecol. Lett., 20, 539–553.
690 Gutiérrez, E. (1991). Climate-tree-growth relationships for *Pinus uncinata* Ram. in the
691 Spanish pre-Pyrenees. Acta Oecol., 12, 213-225.
692 Gutiérrez, E., Campelo, F., Camarero, J.J., Ribas, M., Muntán, E., Nabais, C., et al.
693 (2011). Climate controls act at different scales on the seasonal pattern of *Quercus*
694 *ilex* L. stem radial increments in NE Spain. Trees, 25, 637–646.
695 Haurwitz, M.W., & Brier, G.W., 1981. A critique of the superposed epoch analysis
696 method: its application to solar–weather relations. Mon. Weather. Rev., 109, 2074–
697 2079.
698 Huang, M., Wang, X., Keenan, T.F. & Piao, S. (2018). Drought timing influences the
699 legacy of tree growth recovery. Glob. Chang. Biol., 24, 3546–3559.

Jiang, P., Liu, H., Piao, S., Ciais, P., Wu, X., Yin, Y., et al. (2019). Enhanced growth after extreme wetness compensates for post-drought carbon loss in dry forests. Nat. Commun., 10, 195. doi: 10.1038/s41467-018-08229-z

Kannenberg, S.A., Novick, K.A., Alexander, M.R., Maxwell, J.T., Moore, D.J., Phillips, R.P., et al. (2019a). Linking drought legacy effects across scales: From leaves to tree rings to ecosystems. Glob. Chang. Biol., 25, 2978–2992.

Kannenberg, S.A., Maxwell, J.T., Pederson, N., D'Orangeville, L., Ficklin, D.L. & Phillips, R.P. (2019b). Drought legacies are dependent on water table depth, wood anatomy and drought timing across the eastern US. Ecol. Lett., 22, 119–127.

Leuzinger, S., Zotz, G., Asshoff, R. & Körner, C. (2005). Responses of deciduous forest trees to severe drought in Central Europe. Tree Physiol., 25, 641–650.

Linares, J.C., Camarero, J.J. & Carreira, J.A. (2010). Competition modulates the adaptation capacity of forests to climatic stress: insights from recent growth decline and death in relict stands of the Mediterranean fir *Abies pinsapo*. J. Ecol., 185, 471–480.

Lough, J.M. & Fritts, H.C. (1987). An assessment of the possible effects of volcanic eruptions on North American climate using tree-ring data, 1602 to 1900 A.D. Clim. Ch. 10, 219–239.

Martin-Hernandez, N., Vicente-Serrano, S.M., Azorin-Molina, C., Begueria-Portugues, S., Reig-Gracia, F. & Zabalza-Martınez, J. (2017). Long-term vegetation activity trends in the Iberian Peninsula and The Balearic Islands using high spatial resolution NOAA-AVHRR data (1981–2015). Geophys. Res. Abstr., 19, EGU2017, 16636.

Martín Vide, J. & Olcina, J. (2001). *Climas y Tiempos de España*, Alianza Editorial, Madrid, 258 pp.

Nakagawa, S. & Schielzeth, H. (2013). A general and simple method for obtaining $R^2$ from generalized linear mixed-effects models. Methods Ecol. Evol., 4, 133–142.

Nehrbass-Ahles, C., Babst, F., Klesse, S., Nötzli, M., Bouriaud, O., Neukom, R., et al. (2014). The influence of sampling design on tree-ring-based quantification of forest growth. Glob. Chang. Biol., 20, 2867–2885.

Orwig, D. A., & Abrams, M. D. (1997). Variation in radial growth responses to drought among species, site, and canopy strata. Trees, 11, 474–484.

Pacheco, A., Camarero, J.J., Ribas, M., Gazol, A., Gutiérrez, E. & Carrer, M. (2018). Disentangling the climate-driven bimodal growth pattern in coastal and continental Mediterranean pine stands. Sci. Total Environ., 15, 1518–1526.

Pasho, E., Camarero, J.J., de Luis, M. & Vicente-Serrano, S.M. (2011). Impacts of drought at different time scales on forest growth across a wide climatic gradient in north-eastern Spain. Agric. For. Meteorol., 151, 1800–1811.

Peltier, D.M. & Ogle, K. (2019a). Legacies of La Niña: North American monsoon can rescue trees from winter drought. Glob. Chang. Biol., 25, 121–133.

Peltier, D.M. & Ogle, K. (2019b). Legacies of more frequent drought in ponderosa pine across the western United States. Glob. Chang. Biol., 25, 3803–3816.

Peltier, D.M.P., Barber, J.J. & Ogle, K. (2017). Quantifying antecedent climatic drivers of tree growth in the Southwestern US. J. Ecol., 106, 613–624.

Peltier, D.M.P., Fell, M. & Ogle, K. (2016). Legacy effects of drought in the southwestern United States: A multi-species synthesis. Ecol. Monogr., 86, 312–326.

Pinheiro, J.C. & Bates, D.M. (2000). *Mixed Effects Models in S and S-Plus*. Springer, New York, USA, 548 pp.

749 Pinheiro, J., Bates, D., DebRoy, S., Sarkar, D. & R Core Team (2014). nlme: Linear and
750 Nonlinear Mixed Effects Models. R package version 3.1-117.
751 R Core Team. (2018). R: A language and environment for statistical computing. R
752 Foundation for Statistical Computing, Vienna, Austria.
753 Rao, M.P., Cook, E.R., Cook, B.I., Anchukaitis, K.J., D'Arrigo, R., Krusic, P.J. &
754 LeGrande, A.N. (2019). A double bootstrap approach to Superposed Epoch
755 Analysis to evaluate response uncertainty. Dendrochronologia 55, 119–124.
756 Rossi, S., Deslauriers, A., Anfodillo, T., Morin, H., Saracino, A., Motta, R., et al.
757 (2006). Conifers in cold environments synchronize maximum growth rate of tree-
758 ring formation with day length. New Phytol., 170, 301–310.
759 Sangüesa-Barreda, G., Camarero, J.J., Oliva, J., Montes, F. & Gazol, A. (2015). Past
760 logging, drought and pathogens interact and contribute to forest dieback. Agric.
761 For. Meteorol, 208, 85–94.
762 Sánchez-Salguero, R., Camarero, J.J., Carrer, M., Gutiérrez, E., Alla, A.Q., Andreu-
763 Hayles, L. et al. (2017). Climate extremes and predicted warming threaten
764 Mediterranean Holocene firs forests refugia. Proc. Natl. Acad. Sci. U.S.A., 114,
765 E10142–E10150.
766 Sánchez-Salguero, R., Camarero, J.J., Rozas, V., Génova, M., Olano, J.M., Arzac, A., et
767 al. (2018). Resist, recover or both? Growth plasticity in response to drought is
768 geographically structured and linked to intraspecific variability in Pinus pinaster. J.
769 Biogeogr., 45, 1126– 1139.
770 Schielzeth, H. (2010). Simple means to improve the interpretability of regression
771 coefficients. Methods Ecol. Evol., 1, 103–113.
772 Schweingruber, F.H. (1986). Abrupt growth changes in conifers. IAWA Bulletin, 7,
773 277–283.

774 Serra-Maluquer, X., Gazol, A., Sangüesa-Barreda, G., Sánchez-Salguero, R., Rozas, V.,
775 Colangelo, M., Gutiérrez, E., & Camarero, J.J. (2019). Geographically Structured
776 Growth decline of Rear-Edge Iberian Fagus sylvatica Forests After the 1980s Shift
777 Toward a Warmer Climate. Ecosystems, 22, 1325–1337.
778 Stocker, B.D., Zscheischler, J., Keenan, T.F., Prentice, I.C., Seneviratne, S.I. &
779 Peñuelas, J. (2019). Drought impacts on terrestrial primary production
780 underestimated by satellite monitoring. Nat. Geosci., 12, 264–270.
781 Tucker, C.J. (1979). Red and photographic infrared linear combinations for monitoring
782 vegetation. Remote Sens. Environ., 8, 127–150.
783 Vicente-Serrano, S.M., Beguería, S., López-Moreno, J.I. (2010). A multiscalar drought
784 index sensitive to global warming: the stamdardized precipitation
785 evapotranspiration index. J. Clim. 23, 1696–1718.
786 Vicente-Serrano, S.M., Gouveia, C., Camarero, J.J., Beguería, S., Trigo, R., López-
787 Moreno, J.I., et al. (2013). Response of vegetation to drought time-scales across
788 global land biomes. Proc. Natl. Acad. Sci. U.S.A., 110, 52–57.
789 Vicente-Serrano, S.M., Lopez-Moreno, J.I., Beguería, S., Lorenzo-Lacruz, J., Sanchez-
790 Lorenzo, A., García-Ruiz, J.M., et al. (2014). Evidence of increasing drought
791 severity caused by temperature rise in southern Europe. Environ. Res. Lett., 9,
792 044001. doi:10.1088/1748-9326/9/4/044001
793 Vicente-Serrano, S.M., Tomas-Burguera, M., Beguería, S., Reig, F., Latorre, B., Peña-
794 Gallardo, M., et al. (2017). A high-resolution dataset of drought indices for Spain.
795 Data, 2, 22. doi: 10.3390/data2030022
796 Vicente-Serrano, S. M., Martín-Hernández, N., Camarero, J. J., Gazol, A., Sánchez-
797 Salguero, R., Peña-Gallardo, M., et al. (2020). Linking tree-ring growth and

satellite-derived gross primary growth in multiple forest biomes. Temporal-scale matters. Ecol. Indic., 108, 105753.

Vilà-Cabrera, A. & Jump, A.S. (2019). Greater growth stability of trees in marginal habitats suggests a patchy pattern of population loss and retention in response to increased drought at the rear edge. Ecol. Lett., 22, 1439–1448.

Wood, S.N. (2017). *Generalized Additive Models: An Introduction with R*. 2nd Ed. Chapman & Hall-CRC Press, Boca Raton, USA, 410 pp.

Zhang, Z., Babst, F., Bellassen, V., Frank, D., Launois, T., Tan, K., et al. (2017). Converging climate sensitivities of European forests between observed radial tree growth and vegetation models. Ecosystems, 21, 410–425.

809 **Supporting Information**

810 Additional Supporting Information may be found in the online version of this article:

811 **Figure S1.** Geographical distribution of the sampled tree species and forests.

812 **Figure S2.** Calculation of NDVI legacies.

813 **Figure S3.** Temporal patterns of RWI and NDVI for the different species.

814 **Figure S4.** Impacts of drought on growth at different time scales.

815 **Figure S5.** Impacts of drought on NDVI at different time scales.

816 **Figure S6.** Occurrence of drought events across sites.

817 **Figure S7.** Effect of the interaction between growth variability and tree species on
818 second-year RWI legacies.

819 **Figure S8.** Effect of the interaction between growth variability and tree species on
820 third-year RWI legacies.

821 **Figure S9.** Effect of water balance on second-year NDVI legacies.

822 **Figure S10.** Effect of the interaction between water balance and tree species on third-
823 year NDVI legacies.

824 **Table S1.** Sites displaying negative legacies in RWI and NDVI across species.

825 **Table S2.** Correlation between RWI and NDVI legacies.

826 **Table S3.** Model selection table for RWI drought legacies.

827 **Table S4.** Model selection table for NDVI drought legacies.

828

**Supporting Information**

Manuscript title: **Drought legacies are short, prevail in dry conifer forests and depend on growth variability**

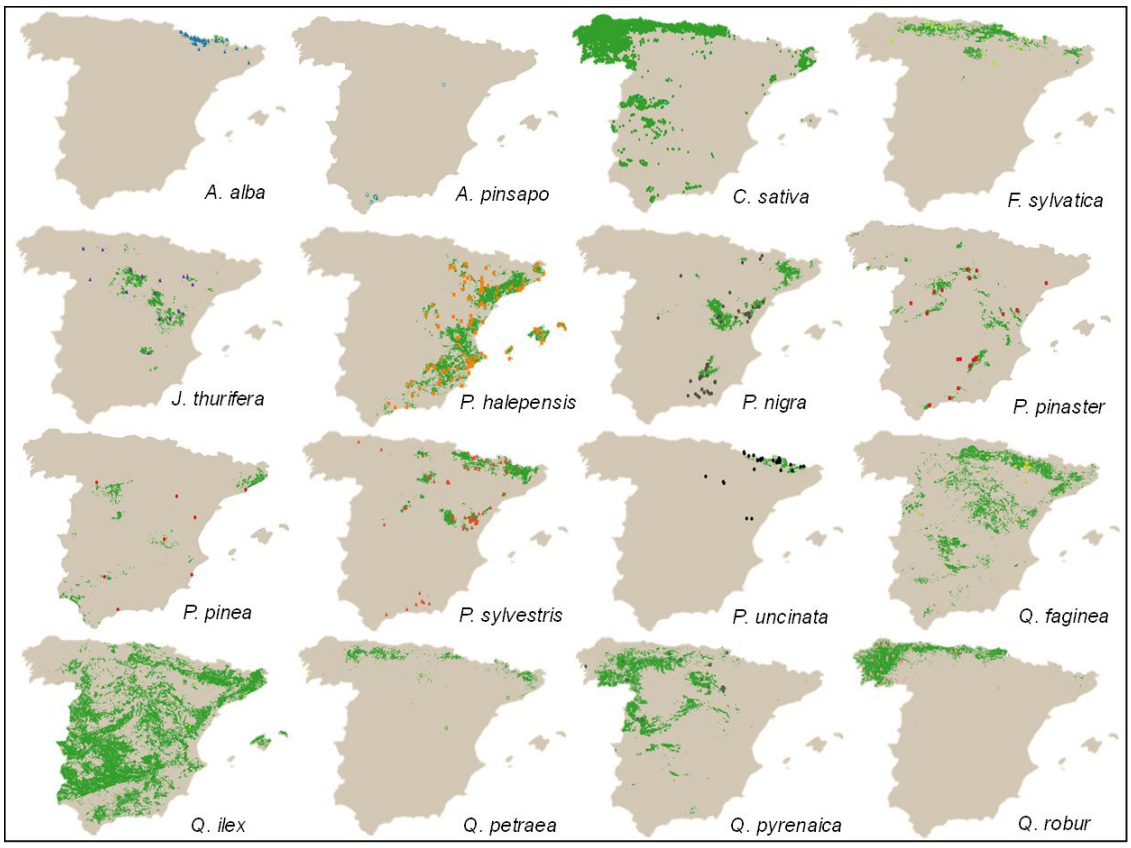


**Figure S1.** Maps showing the distribution in Spain of the sampled tree species (green areas) and the sampled forests (points of different colors). Note how some tree species are restricted either to the wettest sites in the north and north-west Iberia (e.g., *Quercus robur*) or to the driest sites in the east and south-east Iberia (e.g., *Pinus halepensis*).

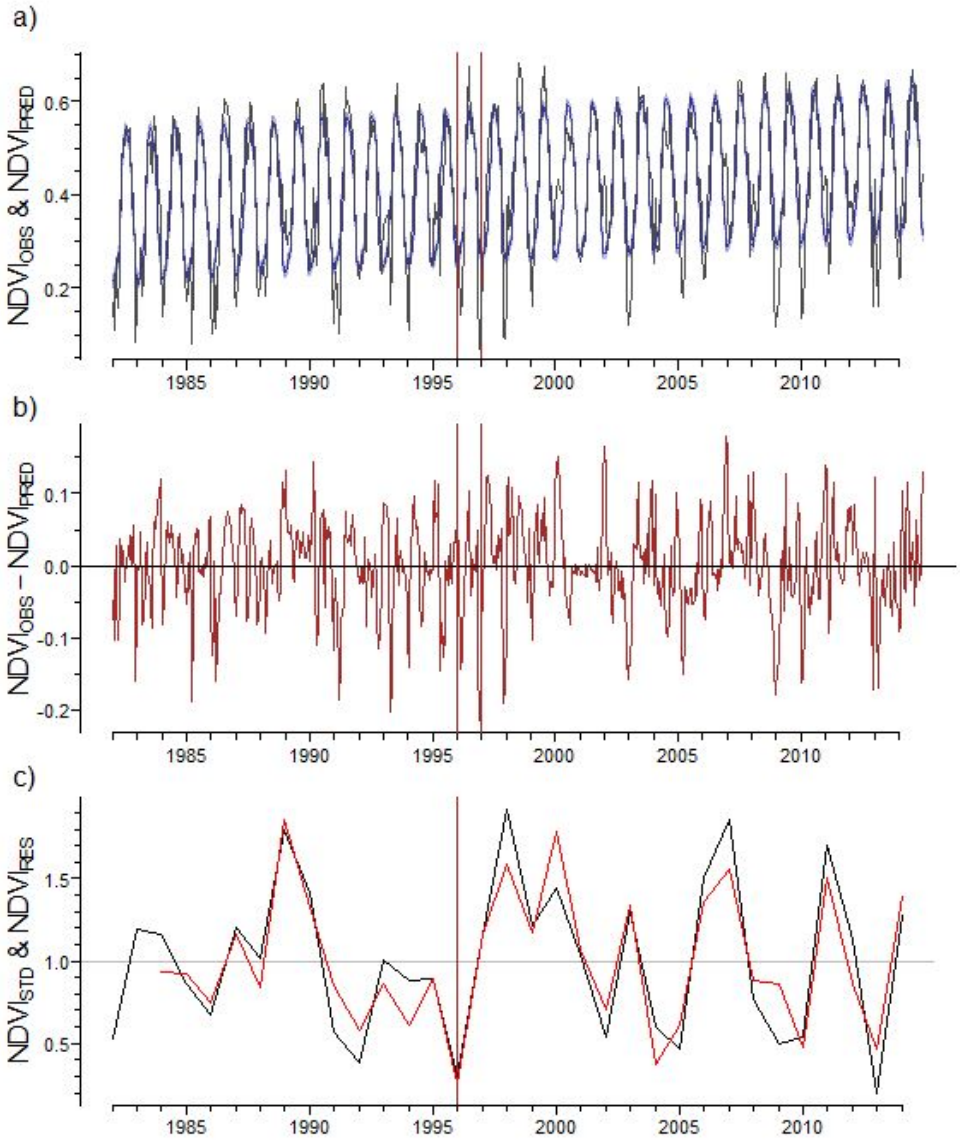


**Figure S2.** Graphical representation of the method used to calculate $NDVI_{STD}$ and $NDVI_{RES}$. In plot (a) the observed (grey) and fitted (blue) NDVI for the period 1982–2014 at biweekly resolution are shown. A Generalized Additive Mixed Model (GAMM) was used to represent the long-term and intra-annual variation in NDVI. In plot (b) the residual variation was calculated as the difference between observed NDVI ($NDVI_{OBS}$) and NDVI predicted by the GAMM ($NDVI_{PRED}$). Finally, the resulting residuals (c) were averaged for every year (black line) and scaled to mean = 1 to obtain standardized NDVI ( $NDVI_{STD}$), and detrended to remove temporal autocorrelation and to obtain pre-whitened o residual NDVI data ($NDVI_{RES}$).

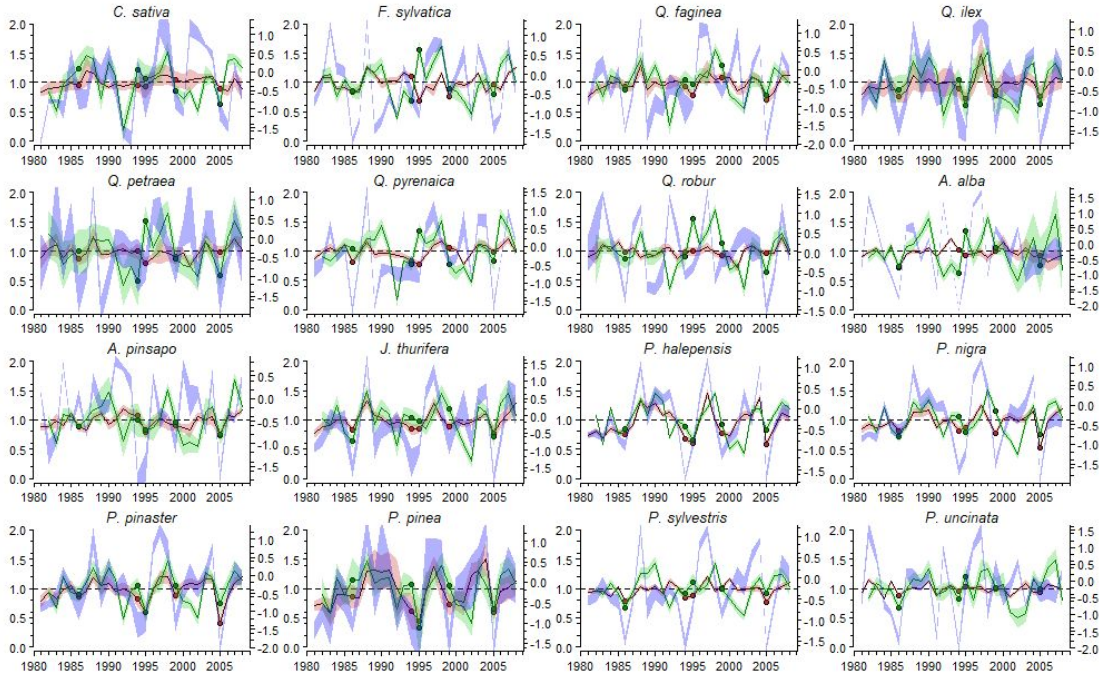


**Figure S3.** Standardized growth (RWI, ring-width index) and forest productivity (NDVI) and their variation between years. RWI is represented with red dots (common droughts), black lines (mean RWI values) and pink shaded areas (95 % confidence interval). NDVI is represented with green dots, lines and shaded areas. Finally, the SPEI for the site is represented with blue shaded areas.

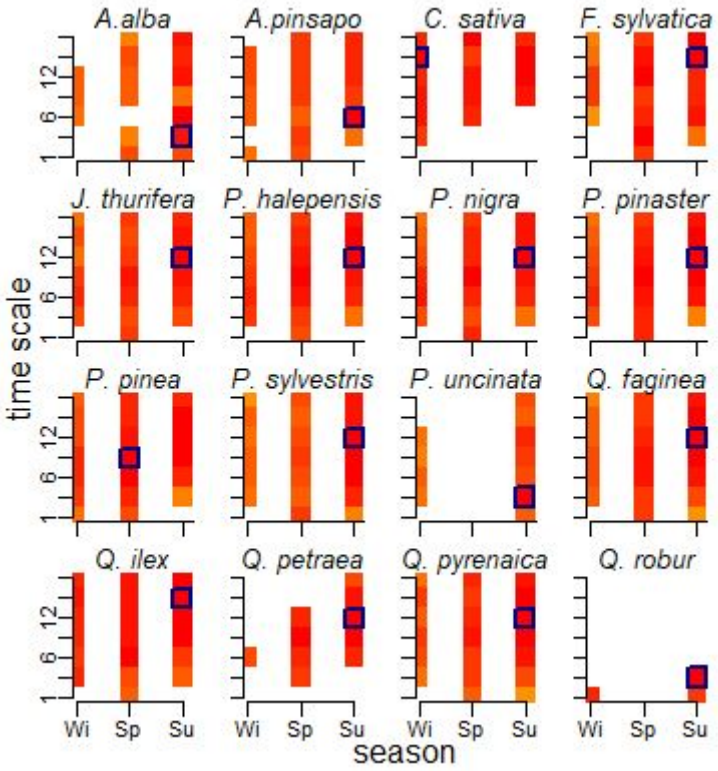


**Figure S4.** Relationships between pre-whitened chronologies ($RWI_{RES}$) and SPEI at different time scales and calculated for different seasons (Wi, previous winter; Sp, spring; Su, summer). Coloured squares indicate the presence of significant positive relationships between $RWI_{RES}$ and the SPEI. The blue box is used to indicate the SPEI timescale and season displaying the lowest AICc value and selected for each species.

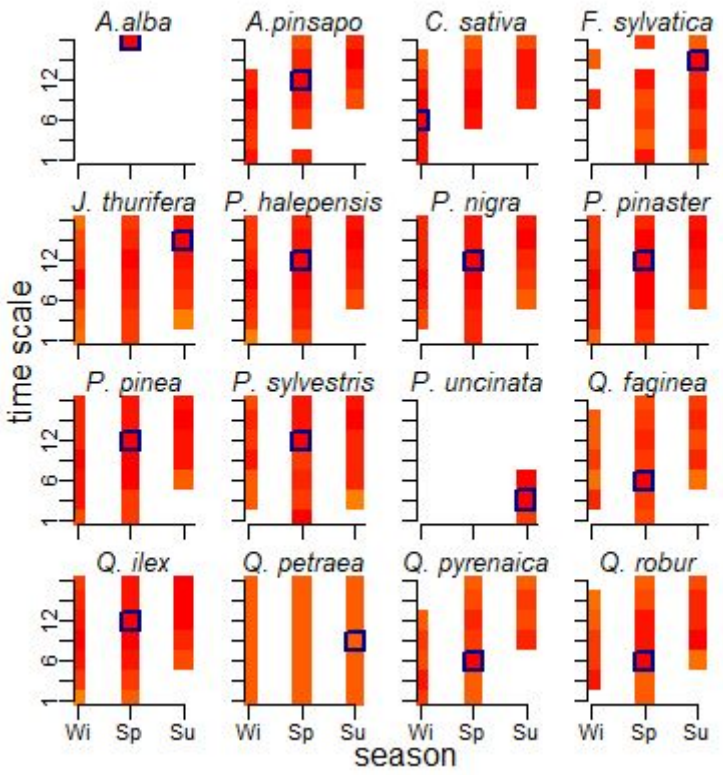


**Figure S5.** Relationships between pre-whitened NDVI time-series ($NDVI_{RES}$) and SPEI at different time scales and calculated for different seasons (Wi, previous winter; Sp, spring; Su, summer). Coloured squares indicate the presence of significant positive relationships between $RWI_{RES}$ and the SPEI. The blue box is used to indicate the SPEI timescale and season displaying the lowest AICc value and selected for each species.

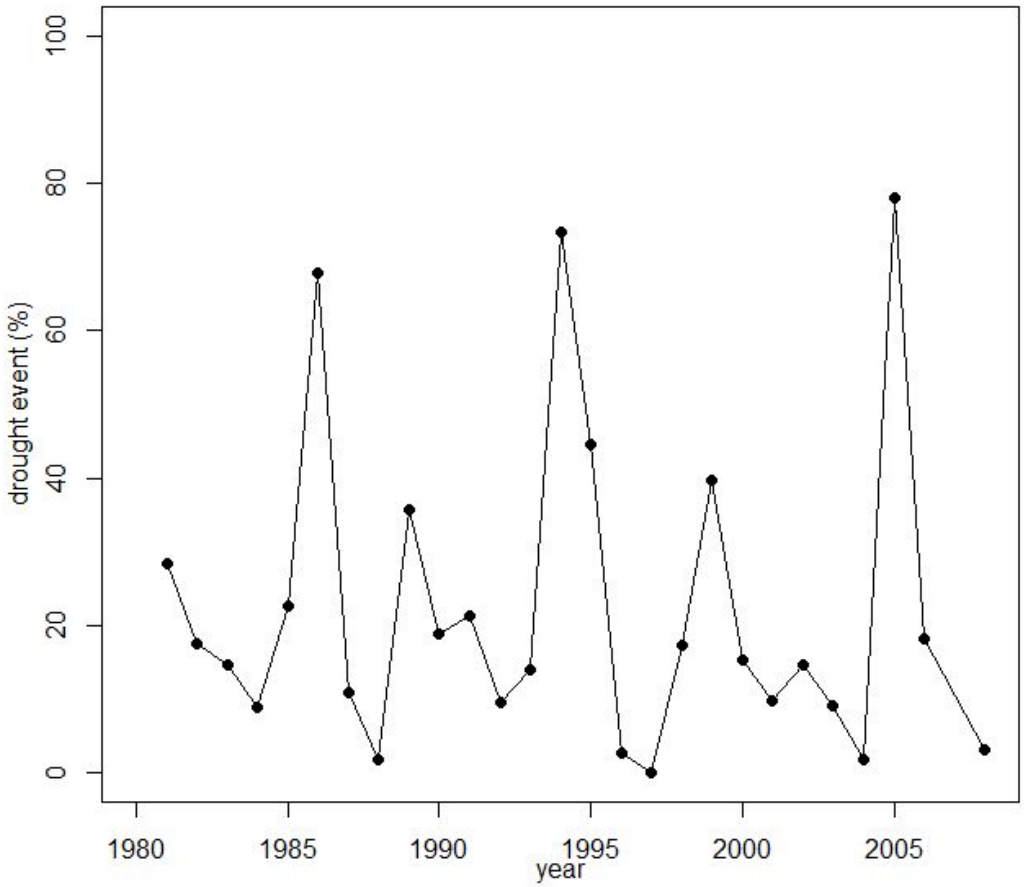


**Figure S6.** Occurrence of drought events across sites. The figure shows the percentage of sites in which each particular year was selected as a drought event for having SPEI values in the lowest 20% percentile.

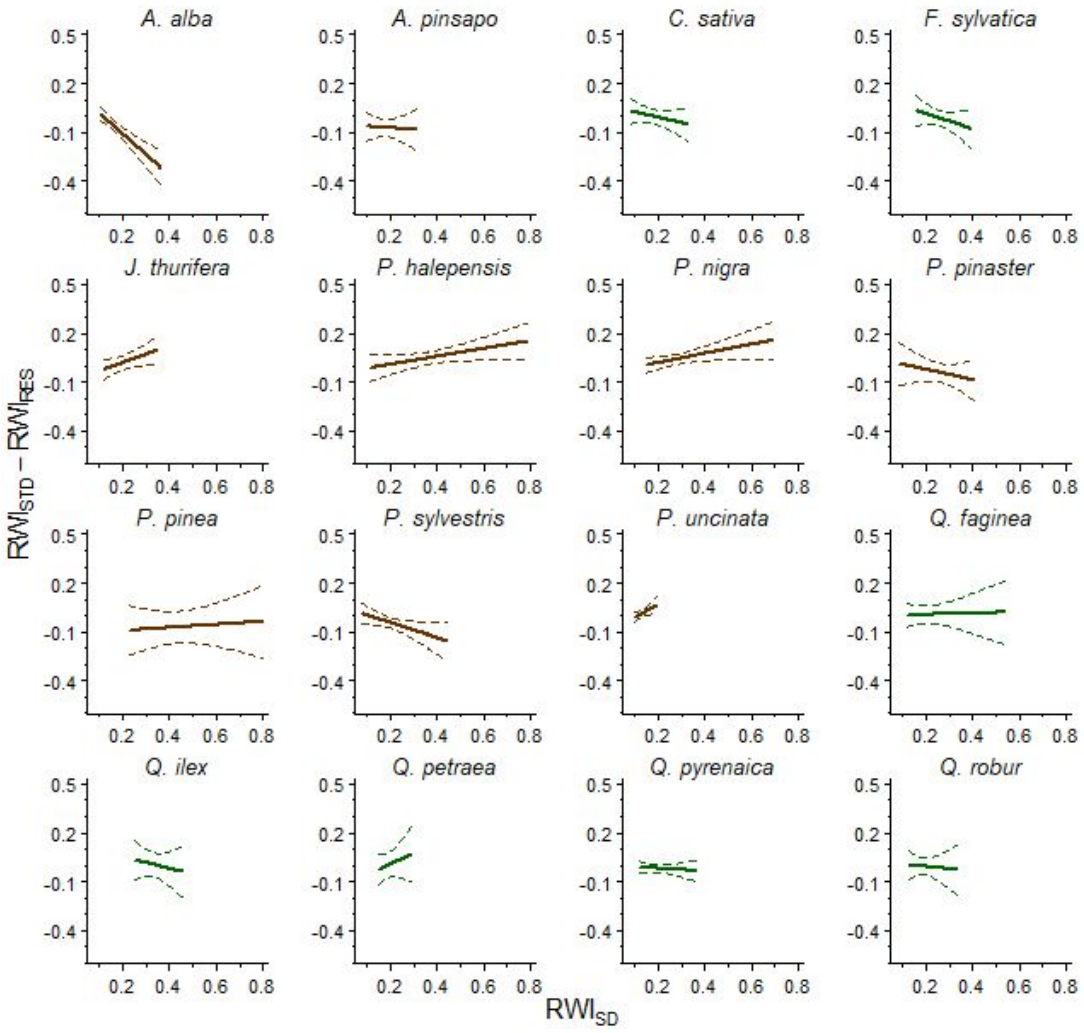


**Figure S7.** Variation of post-drought RWI legacies ($RWI_{STD}$–$RWI_{RES}$) in the second year after drought between species and according to growth variability ($RWI_{SD}$). For each species, the line represents the regression slope for the relationship between growth variability ($RWI_{SD}$) and second-year legacies and the dashed lines are the 95% confidence intervals of the prediction.

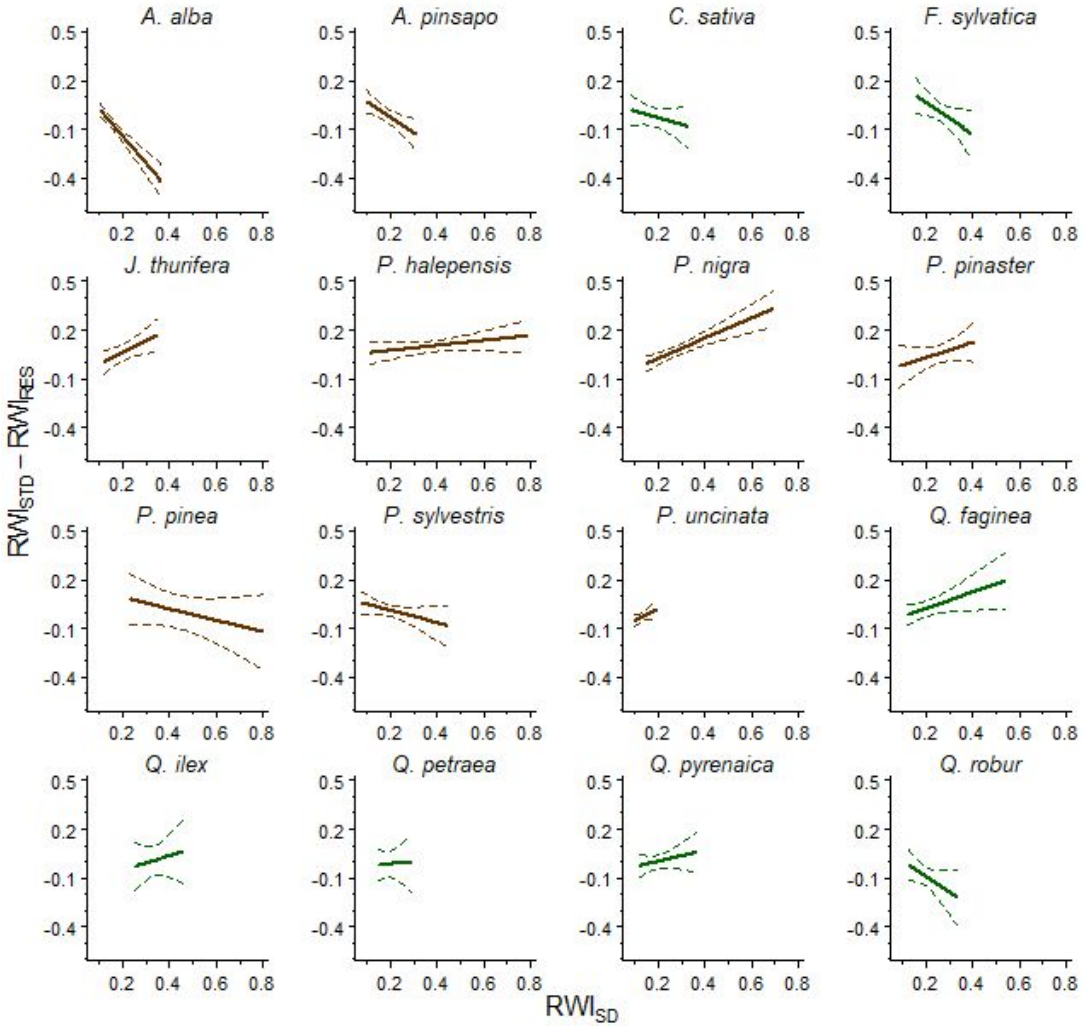


**Figure S8.** Variation of post-drought RWI legacies ($RWI_{STD} - RWI_{RES}$) in the third year after drought between species and according to growth variability ($RWI_{SD}$). For each species, the line represents the regression slope for the relationship between growth variability ($RWI_{SD}$) and third-year legacies and the dashed lines are the 95% confidence intervals of the prediction.

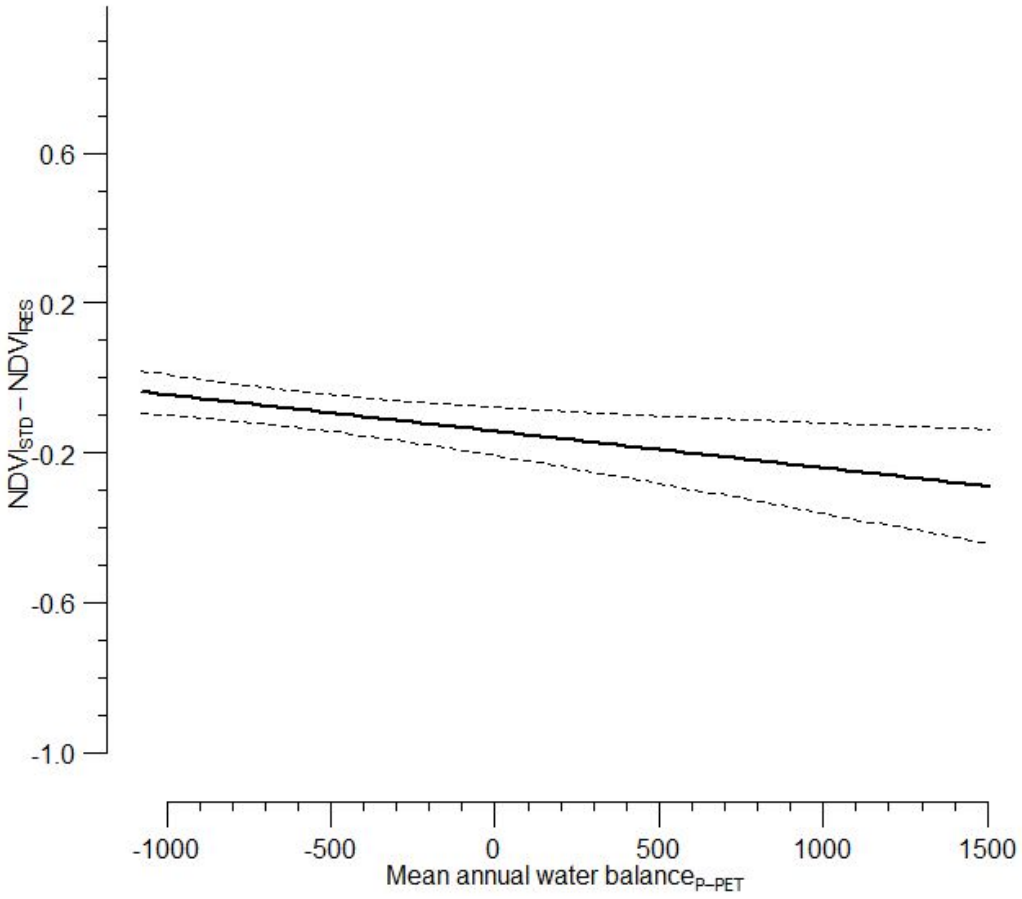


**Figure S9.** Variation of post-drought NDVI legacies ($NDVI_{STD}$ –$NDVI_{RES}$) in the second year after drought between species and according to mean annual water balance (P–PET, in mm). The line represents the regression slope for the relationship between mean annual water balance and second-year NDVI legacies and the dashed lines are the 95% confidence intervals of the prediction.

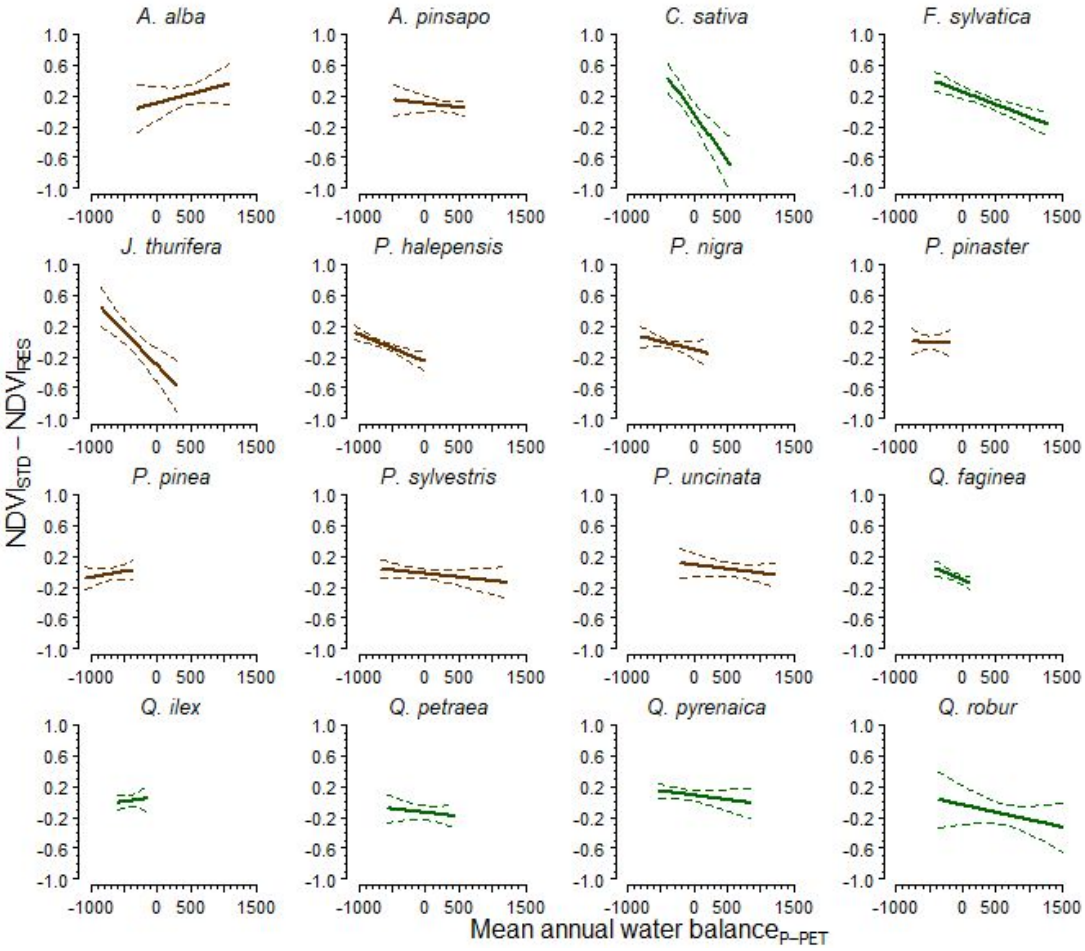


**Figure S10.** Variation of post-drought NDVI legacies ($NDVI_{STD}$ –$NDVI_{RES}$) in the third year after drought between species and according to mean annual water balance (P–PET, in mm). For each species, the line represents the regression slope for the relationship between mean annual water balance and third-year legacies and the dashed lines are the 95% confidence intervals of the prediction.

**Table S1.** Percentage of sites displaying negative legacies in RWI and NDVI from one (e.g. RWI 1) up to three (e.g. RWI 3) years after drought occurrence.

| | Growth legacies | | | NDVI legacies | | |
|---|---|---|---|---|---|---|
| Tree species (code) | *year 1* | *year 2* | *year 3* | *year 1* | *year 2* | *year 3* |
| *Abies alba* (ABAL) | 88.6 | 65.9 | 70.5 | 50.0 | 43.2 | 25.0 |
| *Abies pinsapo* (ABPN) | 91.7 | 83.3 | 50.0 | 100.0 | 66.7 | 33.3 |
| *Castanea sativa* (CASA) | 60.0 | 60.0 | 40.0 | 20.0 | 30.0 | 20.0 |
| *Fagus sylvatica* (FASY) | 60.4 | 52.1 | 43.8 | 6.3 | 31.3 | 29.2 |
| *Juniperus thurifera* (JUTH) | 66.7 | 46.7 | 33.3 | 33.3 | 60.0 | 66.7 |
| *Pinus halepensis* (PIHA) | 68.0 | 37.0 | 28.0 | 70.0 | 61.0 | 61.0 |
| *Pinus nigra* (PINI) | 59.3 | 40.7 | 30.5 | 71.2 | 71.2 | 55.9 |
| *Pinus pinaster* (PIPI) | 77.8 | 66.7 | 33.3 | 66.7 | 44.4 | 55.6 |
| *Pinus pinea* (PIPN) | 100.0 | 66.7 | 55.6 | 88.9 | 66.7 | 66.7 |
| *Pinus sylvestris* (PISY) | 60.7 | 65.6 | 42.6 | 50.8 | 52.5 | 59.0 |
| *Pinus uncinata* (PIUN) | 73.1 | 46.2 | 73.1 | 61.5 | 73.1 | 53.8 |
| *Quercus faginea* (QUFA) | 66.7 | 44.4 | 44.4 | 33.3 | 38.9 | 77.8 |
| *Quercus ilex* (QUIL) | 78.6 | 50.0 | 42.9 | 42.9 | 57.1 | 42.9 |
| *Quercus petraea* (QUPE) | 40.0 | 60.0 | 40.0 | 20.0 | 80.0 | 100.0 |
| *Quercus pyrenaica* (QUPY) | 71.9 | 62.5 | 53.1 | 9.4 | 18.8 | 37.5 |
| *Quercus robur* (QURO) | 55.2 | 48.3 | 72.4 | 65.5 | 79.3 | 75.9 |

87 **Table S2.** Pearson correlation coefficients calculated by relating post-drought growth
88 ($RWI_{STD}$ –$RWI_{RES}$) and NDVI legacies ($NDVI_{STD}$ –$NDVI_{RES}$) from one to three years
89 after drought. The significance ($p < 0.01$) is indicated with asterisks (**).
90

| Growth | *year 2* | *year 3* |
|---|---|---|
| *year 1* | 0.61** | 0.45** |
| *year 2* | | 0.68** |
| NDVI | | |
| *year 1* | 0.65** | 0.44** |
| *year 2* | | 0.62** |

91
92

**Table S3.** Summary of model selection statistics and variables used to explain the variation in post-drought RWI legacies ($RWI_{STD} - RWI_{RES}$). For the legacies in one to three years after drought occurrence, the best ten models ranked according to its second order Akaike information criterion (AICc) are shown. The variables included in the model (with their standardized coefficient) and the ΔAICc (i.e. the difference in AICc as compared to the "best" model) are shown. The selected model is highlighted in bold. Variables are tree species (factor 16 levels); mean annual water balance (WB); growth variability ($RWI_{SD}$); growth persistence ($RWI_{AR}$) and their interactions. The ∑ Akaike weights represent the probability (in a 0 – 1 scale) that the selected models are the best set of models to explain variation in the response variable.

| | Intercept | Tree species | WB | $RW_{SD}$ | $RWI_{AR}$ | Tree species:WB | Tree species: $RW_{SD}$ | Tree species: $RWI_{AR}$ | WB: $RW_{SD}$ | WB: $RWI_{AR}$ | ΔAICc | Akaike weight |
|---|---|---|---|---|---|---|---|---|---|---|---|---|
| *year 1* | -0.17 | + | 0.01 | -0.07 | | | + | | | | 0.00 | 0.3 |
| | **-0.16** | **+** | | **-0.07** | | | **+** | | | | **0.18** | **0.27** |
| | -0.18 | + | 0.02 | -0.08 | | | + | | 0.01 | | 2.09 | 0.11 |
| | -0.17 | + | 0.01 | -0.07 | 0.00 | | + | | | | 2.39 | 0.09 |
| | -0.16 | + | | -0.07 | 0.00 | | + | | | | 2.60 | 0.08 |
| | -0.17 | + | 0.02 | -0.08 | 0.00 | | + | | 0.01 | | 4.46 | 0.03 |
| | -0.17 | + | 0.01 | -0.07 | 0.00 | | + | | | 0.00 | 4.82 | 0.03 |
| | -0.14 | + | 0.03 | | | + | | | | | 5.58 | 0.02 |
| | -0.18 | + | 0.03 | -0.07 | | + | + | | | | 6.44 | 0.01 |

| | | | | | | | | | | | | | |
|---|---|---|---|---|---|---|---|---|---|---|---|---|---|
| | -0.16 | + | | -0.09 | 0.01 | | + | + | | | | 6.70 | 0.01 |
| *year 2* | **-0.18** | **+** | | **-0.16** | | | **+** | | | | | **0.00** | 0.17 |
| | -0.05 | + | -0.06 | -0.03 | | + | | | -0.05 | | | 0.80 | 0.12 |
| | -0.12 | + | -0.06 | -0.13 | | + | + | | -0.03 | | | 1.22 | 0.09 |
| | -0.15 | + | -0.03 | -0.17 | | + | + | | | | | 1.24 | 0.09 |
| | -0.17 | + | | -0.16 | 0.00 | | + | | | | | 1.83 | 0.07 |
| | -0.18 | + | 0.00 | -0.16 | | | + | | | | | 2.21 | 0.06 |
| | -0.07 | + | -0.02 | -0.02 | | | | | -0.03 | | | 3.07 | 0.04 |
| | -0.05 | + | -0.06 | -0.03 | 0.00 | + | | | -0.04 | | | 3.23 | 0.03 |
| | -0.17 | + | -0.01 | -0.14 | | | + | | -0.02 | | | 3.43 | 0.03 |
| | -0.17 | + | 0.00 | -0.15 | 0.00 | | + | | | -0.01 | | 3.84 | 0.03 |
| *year 3* | -0.21 | + | -0.02 | -0.22 | | | + | | | | | 0.00 | 0.39 |
| | **-0.23** | **+** | | **-0.21** | | | **+** | | | | | **1.68** | **0.17** |
| | -0.21 | + | -0.02 | -0.21 | 0.00 | | + | | | | | 2.46 | 0.11 |
| | -0.21 | + | -0.02 | -0.21 | | | + | | 0.00 | | | 2.46 | 0.11 |
| | -0.23 | + | | -0.21 | 0.00 | | + | | | | | 4.12 | 0.05 |

| | | | | | | | | | | |
|---|---|---|---|---|---|---|---|---|---|---|
| -0.20 | + | -0.02 | -0.21 | 0.00 | | + | | -0.01 | 4.17 | 0.05 |
| -0.21 | + | -0.02 | -0.21 | 0.00 | | + | 0.00 | | 4.93 | 0.03 |
| -0.16 | + | -0.06 | -0.17 | | + | + | -0.04 | | 5.73 | 0.02 |
| -0.20 | + | -0.03 | -0.22 | | + | + | | | 6.23 | 0.02 |
| -0.20 | + | -0.02 | -0.21 | 0.00 | | + | 0.00 | -0.01 | 6.63 | 0.01 |

**Table S4.** Summary of model selection statistics and variables used to explain the variation in post-drought NDVI legacies ($NDVI_{STD} - NDVI_{RES}$). For the legacies in one to three years after drought occurrence, the best ten models ranked according to its second order Akaike information criterion (AICc) are shown. The variables included in the model (with their standardized coefficient) and the ΔAICc (i.e. the difference in AIC as compared to the "best" model) are shown. The selected model is highlighted in bold. Variables are tree species (factor 16 levels), mean annual water balance (WB) and its interaction. The ∑ Akaike weights represent the probability (in a 0 – 1 scale) that the selected models are the best set of models to explain variation in the response variable.

| | Intercept | Tree species | WB | Tree species:WB | ΔAICc | Akaike weight |
|---|---|---|---|---|---|---|
| *year 1* | **0.10** | + | **-0.03** | + | **0.00** | 0.99 |
| | 0.11 | + | -0.04 | | 9.48 | 0.01 |
| | 0.07 | + | | | 12.14 | 0.00 |
| | -0.02 | | 0.04 | | 114.57 | 0.00 |
| | -0.03 | | | | 123.02 | 0.00 |
| *year 2* | **0.09** | + | **-0.05** | | **0.00** | 0.92 |
| | 0.04 | + | | | 5.09 | 0.07 |
| | 0.16 | + | -0.13 | + | 10.99 | 0.00 |
| | -0.02 | | | | 36.76 | 0.00 |
| | -0.01 | | 0.00 | | 38.81 | 0.00 |
| *year 3* | **0.08** | + | **0.13** | + | **0.00** | 0.87 |
| | 0.31 | + | -0.10 | | 3.87 | 0.13 |
| | 0.21 | + | | | 32.47 | 0.00 |

| | | | |
|---|---|---|---|
| | -0.01 | 52.65 | 0,00 |

110